Instituto Tecnológico y de Estudios Superiores de Occidente

Reconocimiento de validez oficial de estudios de nivel superior según acuerdo secretarial 15018, publicado en el Diario Oficial de la Federación del 29 de noviembre de 1976.

Departamento de Electrónica, Sistemas e Informática
Maestría en Diseño Electrónico

Upgrade to intelligent module UPU: Power Stage

TRABAJO RECEPCIONAL que para obtener el **GRADO** de
MAESTRO EN DISEÑO ELECTRÓNICO

Presenta: **DIEGO ANDRES GONZALEZ AVALOS**

Director **DR. JUAN RAFAEL DEL REY ACUÑA**

Tlaquepaque, Jalisco. 8 de diciembre de 2025.

To my wife Alejandra.

To my sons Santiago and Fernando.

You are the inspiration and strength in my life.

For being part of this sacrifice during these years and accompanying me in closing this chapter in my life.

To my parents.

This is also in your honor, for what is closing and for what I have gained through this process.

Abstract

The present work shows the design upgrade of an intelligent control module used in home automation systems to manage home devices such a lamps, actuators or motors. The design upgrade and information used in this document have been developed for exclusively academic and educational purposes. The module is part of set of multifunction modules and software tools of the LCN® system (Local Control Network) from the company Issendorff KG. The described module which is called LCN-UPU is a sensor/actuator module which has two switching/dimming electronic outputs for $120V_{AC}$. The outputs can be operated as leading and trailing edge dimmer or in switching operation as zero voltage switch.[1] The design upgrade of the LCN-UPU was based on a partial reverse engineering process, the understanding of the module requirements and the detected needs on the local market (Mexico region). For a better understanding of the LCN-UPU module the upgrade was addressed in two sections: Digital and Power stage, in this work the Power stage is covered. Main upgrade on Power stage is the increase from two to three switching/dimming electronic outputs, additionally two high current outputs are now included to extend the module capabilities.

The design procedure to increase the PCB space availability (required to increase the power outputs) started on the downsizing process of the output transistors and it is described in Chapter 1. Then, a short mention about the relay used to drive the high-power outputs is presented in Chapter 2. A comparison between the previous and the new design is presented in Chapter 3 emphasizing the trade-off between the cost and technical benefits. Finally, new design (schematic & PCB layout) are presented in Chapter 4.

Resumen

El presente trabajo muestra la actualización del diseño de un módulo de control inteligente utilizado en sistemas domóticos para gestionar dispositivos domésticos como lámparas, actuadores o motores. La actualización del diseño y la información utilizada en este documento se han desarrollado exclusivamente con fines académicos y educativos. El módulo forma parte del conjunto de módulos multifunción y herramientas de software del sistema LCN® (Red de Control Local) de la empresa Issendorff KG. El módulo descrito, denominado LCN-UPU, es un módulo sensor/actuador con dos salidas electrónicas de conmutación/atenuación para 120 V_{CA}. Las salidas pueden operar como reguladores de intensidad de flanco de entrada y salida, o como interruptores de tensión cero en conmutación. La actualización del diseño del LCN-UPU se basó en un proceso parcial de ingeniería inversa, la comprensión de los requisitos del módulo y las necesidades detectadas en el mercado local (región de México). Para una mejor comprensión del módulo LCN-UPU, la actualización se abordó en dos secciones: etapa digital y etapa de potencia. En este trabajo se aborda la etapa de potencia. La principal actualización de la etapa de potencia es el aumento de dos a tres salidas electrónicas de conmutación/atenuación, además de incluir dos salidas de alta corriente para ampliar las capacidades del módulo. El procedimiento de diseño para aumentar el espacio disponible en la PCB (necesario para aumentar la potencia de salida) comenzó con la reducción del tamaño de los transistores de salida y se describe en el Capítulo 1. Posteriormente, en el Capítulo 2, se presenta una breve descripción del relé utilizado para controlar las salidas de alta potencia. En el Capítulo 3, se presenta una comparación entre el diseño anterior y el nuevo, destacando la relación coste-beneficio. Finalmente, en el Capítulo 4 se presenta el nuevo diseño (esquemático y diseño de la PCB).

Acknowledgements

The author wishes to express his gratitude to Dr. Rafael del Rey, professor of the Department of Electronics, Systems, and Informatics at ITESO, for his guidance and supervision as master degree thesis director. For providing his counseling through the course of this work even if it seemed a difficult challenge for the author.

He also thanks Dr. Omar Humberto Longoria-Gándara, professor of the Department of Electronics, Systems, and Informatics and coordinator of the master degree program of Electronics Design at ITESO, for his interest, assessment and academic support.

Special thanks to Oswaldo Ramirez, teammate project and also student of the master degree program of Electronics Design, for his initiative and prolific cooperation for this project.

The author also appreciates the collaboration with the company Ingeniería Aplicada Tekger S.A. de C.V. for providing the LCN-UPU devices (designed by Issendorff KG) to carry out this Degree Project (Trabajo de Obtencion de Grado).

Table of Contents

Introduction

Nowadays, technological advances are making possible a fast development of solutions and products in areas like communications, computing and electronics. Derived from IT (Information Technology) which manages the use of computers, storage, networking and physical devices[2], there is an extension term known as "ICT" (Information and Communications Technology) which is used as an umbrella term that includes, among many other things, the control and supervision of technological equipment in homes and buildings. [3]

In a domestic environment, users demands an increase of capabilities to handling home systems (climate control equipment, household appliances, motors and lighting systems). [3]

A basic system used in home automation works in this way:

1. Sensors receive the environmental information (physical or electrical parameters).
2. The environment information is transferred through a transmission line to one or several controllers.
3. The controllers provide the activation signal to the actuators (depending on software or system parameters).

The presented work describes a design upgrade of a controller used to drive lights, LED lighting strips, solenoid valves or any device that requires $120V_{AC}$ (standard electricity AC supply voltage in Mexico). This controller called as "intelligent module" is part of a set of multifunction modules and software tools of the LCN® (Local Control Network) home automation systems from the company Issendorff KG and it has the possibility to be interconnected with other modules through its own communication bus.

The intelligent controller module (which we will mention as LCN-UPU) is a sensor-actuator module for building installation. It has 2 switching/dimming electronic outputs at 120V (300VA), capable of driving 2.5A RMS (Fig. 0-1). The module has two ports: T-Port, for connection of up to 8 keys (conventional keyboard, LCN touch keyboard without display or standard keyboard) and I-Port, for temperature sensors, infrared remote control receivers, transponder receivers or the LCN touch keypad with display. [1]

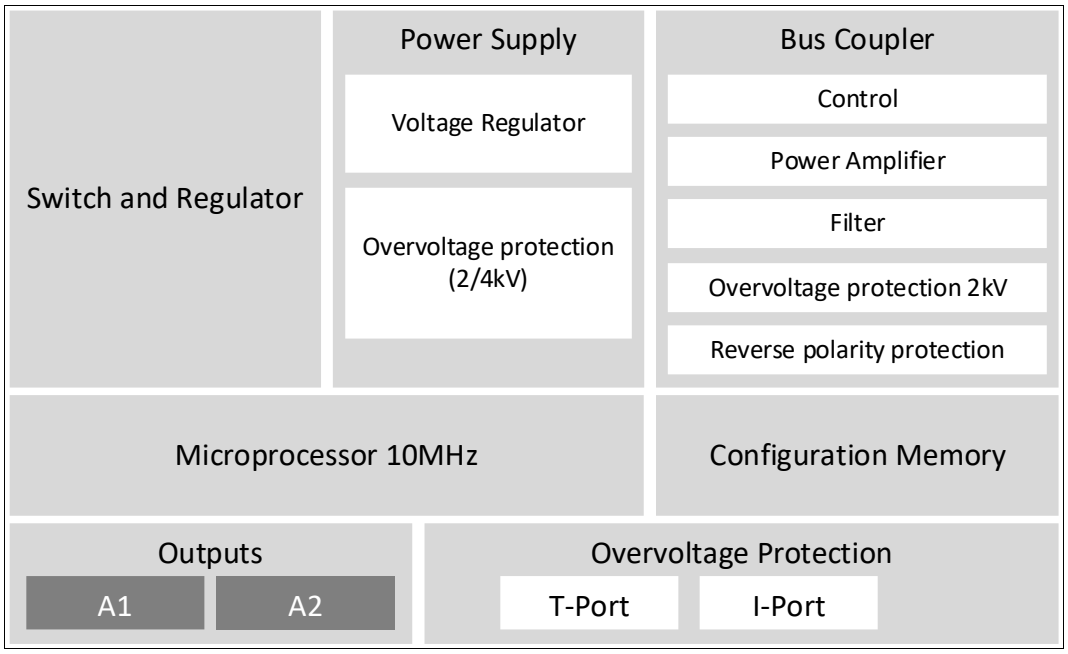

Fig. 0-1 Block diagram of internal architecture of LCN-UPU.

LCN-UPU electrical specifications are shown in Table 1, these values are intended to be used in the local market (México region).

Table 1 LCN-UPU TECHNICAL DATA

Parameter	Value
Power Supply	120VAC ±15%. 50/60Hz
Power Consumption	<0.5W
Load Outputs	2x Zero-voltage switch or phase cut on dimmer
Resolution	200 steps in dimming operation
Switching Capability	300VA (2.5A RMS)
Operating Temperature	-10°C to +60°C

When the LCN-UPU outputs are operated as dimmer, they can handle the two common types of *phase dimming*:

- *Forward phase (Leading edge)* or *Phase cut-on*. In this type of dimming the signal is cut at the front or leading edge of the wavelength.[4] Traditionally used for

incandescent and halogen lamps, in the past this type of dimming was intended for inductive loads driven by TRIACs [5] producing a rush of voltage every half cycle also seen on the light source.[6]

- *Reverse phase (Trailing Edge) or Phase cut-off.* In this type of dimming the signal is now cut at the end or back trailing edge of the wavelength.[4] Today, it is most used for LED lamps and luminaries, in the past it was intended for capacitive loads.[5] Note: If trailing edge is used, the LCN-UPU outputs require an additional external filter.

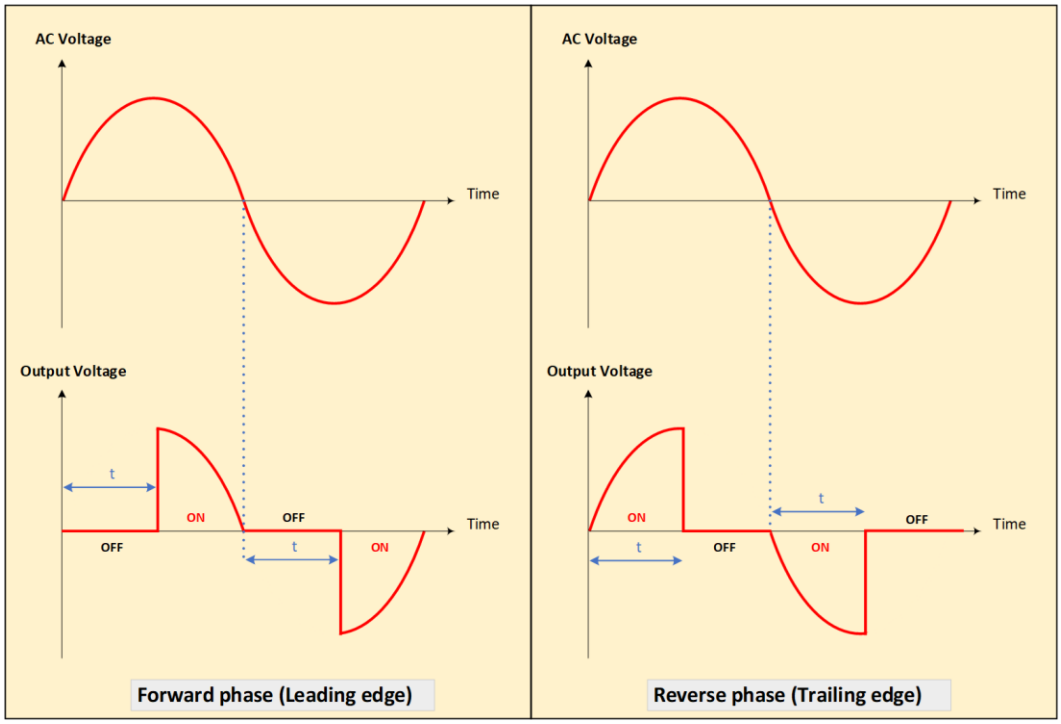

Fig. 0-2 Diagram of Forward phase and Reverse phase dimming.

The design upgrade was addressed in two sections: Digital and Power output stage (Fig. 0-3). This work covers the **Power output stage** portion**.**

In order to be cross-compatible with the reference design platform, in the laboratory, the power stage block was identified and represented through a schematic diagram (Fig. 0-4). All signals identified as *CONN_FLEX_PINx* coming from the left side represent all wire connector which join the digital board with the power output board.

Fig. 0-3 LCNUPU Digital board (left) and Power output board – top side (upper right) & bottom side (lower right).

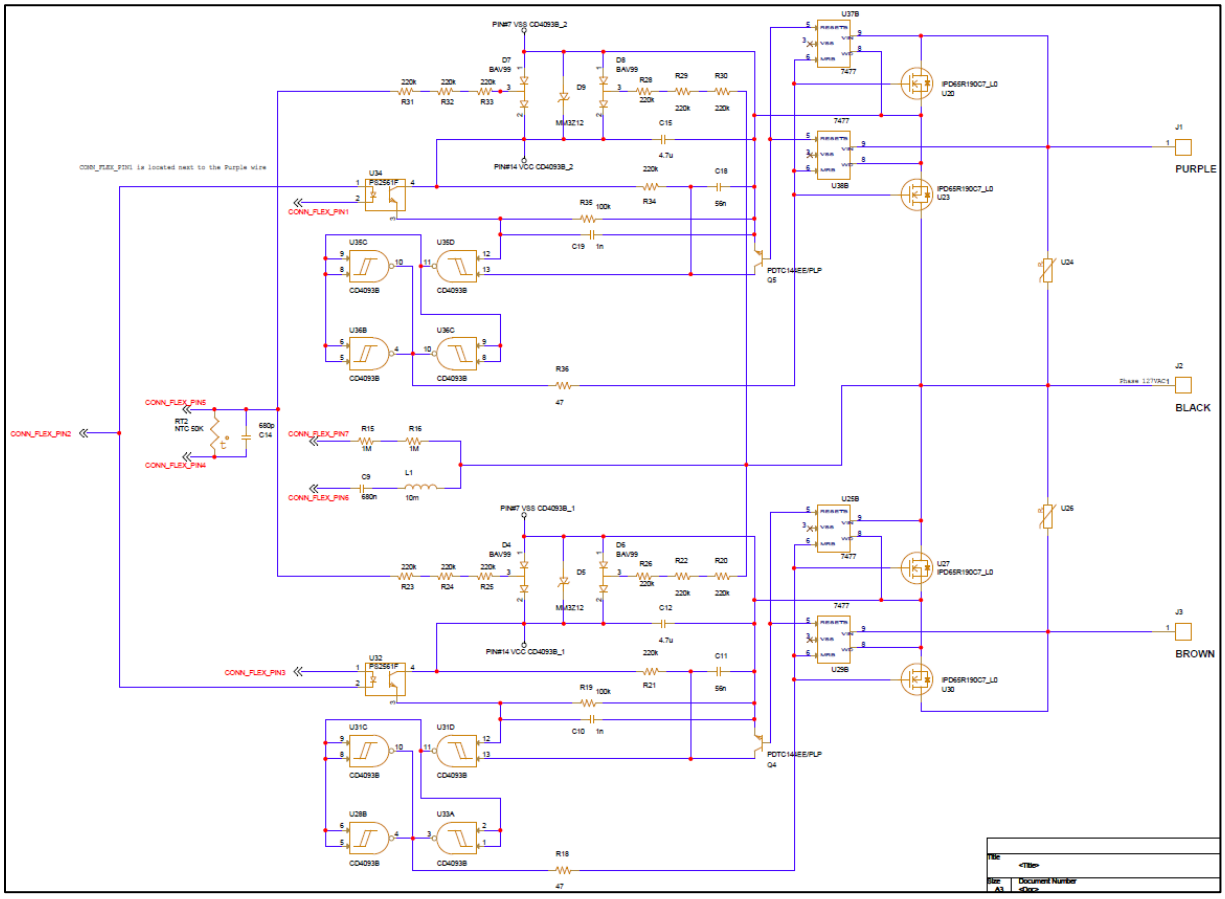

Fig. 0-4 Schematic diagram from LCN-UPU power output stage.

In principle, to drive the AC loads both MOSFETs (N-channel) are connected sharing the source pin and both are turned ON at the same time. This allows one MOSFET to drive the half positive AC voltage signal and the other the half negative AC voltage (Fig. 0-5).

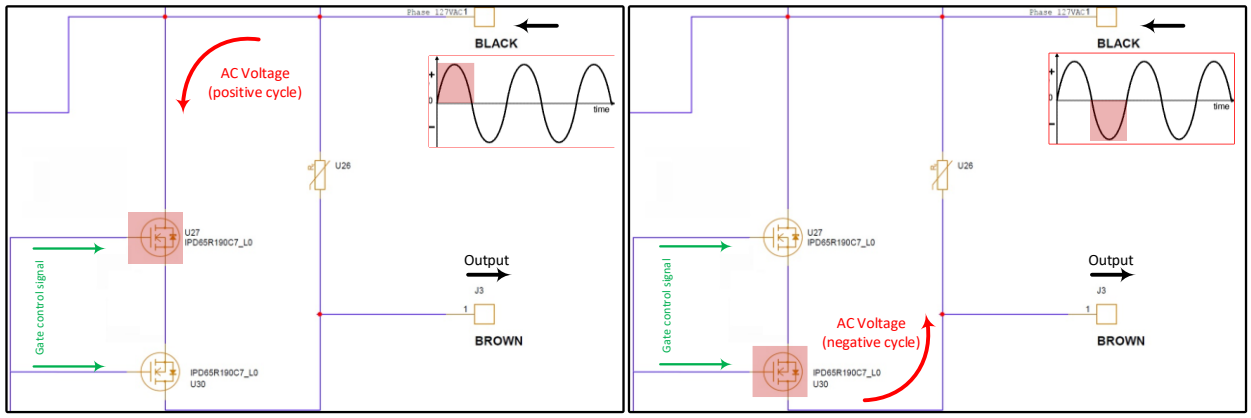

Fig. 0-5 AC voltage driven by N-channel MOSFETs. U27 drives the half positive AC signal (left) and U30 drives the half negative AC signal.

To drive both MOSFETs keeping the proper Vgs voltage this module uses a rectifier bridge circuit (D5 & D6), but in contrast to the traditional bridge this design has a Zener diode (D5) in the half of the bridge. The above creates a voltage difference between the two legs of the bridge and allows them to keep 12V. In other words, *"two AC signals are drawn though every bridge leg"* (same AC phase) only separated by 12V between both signals, so one has an offset of +6V, the other has an offset of -6V with respect to the AC input signal (Fig. 0-6).

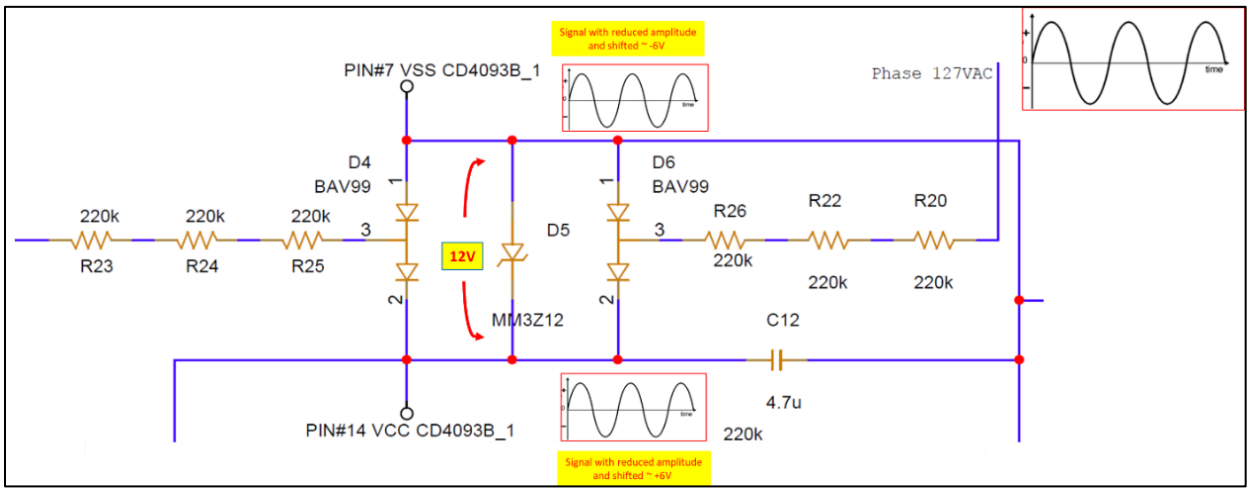

Fig. 0-6 Diode bridge + Zener diode array.

Finally, to reduce the amplitude and current of the waveform, three resistors are placed at the input of the rectified bridge (R26, R22 and R20). The differential voltage (12V) made by the diode bridge + Zener diode is used as reference to supply a logic NAND gate array (U31D, U31C, U28B and U33A), so that the node with an offset of +6V is connected to the VCC pin, in contrast the node with an offset of -6V which is connected to the VSS pin. In this way the signal with the positive offset "is seen" as a HIGH logic state and the signal with the negative offset "is seen" as the LOW logic state.

The purpose to include a NAND gate array is to provide the proper condition to the MOSFET gate control (Fig. 0-7). An optocoupler (U32) is used as the main element of control since it receives a PWM signal coming from the uC, this PWM signal is taken as the input of the optocoupler and the VCC signal (AC) is taken as the output. In this way, the Optocoupler drive the LOW-HIGH state for one of the NAND inputs, and the other NAND input is permanently connected to a HIGH state (VCC).

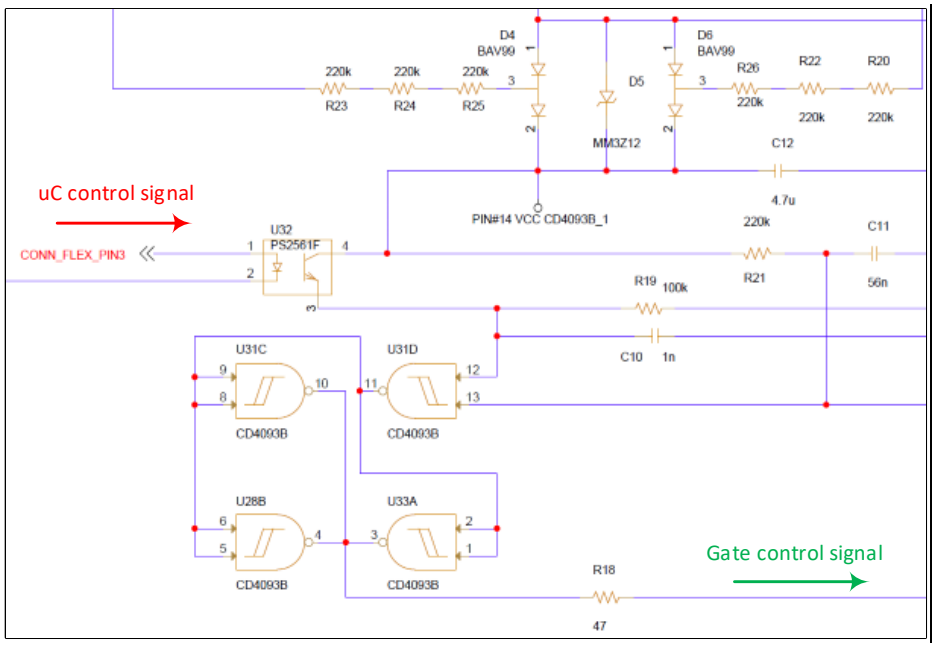

Fig. 0-7 Signal conditioning for MOSFET gate control.

According to the NAND gate array true table (Fig. 0-8) two HIGH states at the input of the first NAND produces a HIGH state at the output of the second NAND and inversely, any combination of HIGH-LOW states at the input of the first NAND produces a LOW state at the second NAND.

NAND U31D				NANDs U31C, U28B, U33A)			
A (12 pin)	B (13 pin)	Q		A	B	Q	
LOW	LOW	HIGH	→	HIGH		LOW	
LOW	HIGH	HIGH	→	HIGH		LOW	
HIGH	LOW	HIGH	→	HIGH		LOW	
HIGH	HIGH	LOW	→	LOW		HIGH	* Mosfet ON

Fig. 0-8 NAND true tables for first and second block.

It's important to highlight that the node identified as VSS (Fig. 0-6) is directly connected to the source MOSFETs common pin, and the gate MOSFETs node is connected to the NAND output array. Therefore, when MOSFET is in OFF state, gate-source pins have the same potential (VSS) seen as Vgs=0V, then when MOSFET is in ON state the gate will reach the VCC potential which is seen as Vgs=12V. The described condition will guarantee the correct ON/OFF MOSFET in any part of the $127V_{AC}$ signal (either negative or positive cycle).

New design proposal: New requirements for power stage board.

The internal architecture block diagram showed in Fig. 0-9 described the complete project design upgrade (Digital and Power board). The scope of this work is:

- Increase from 2 to 3 (A3) switching/dimming electronic outputs driving 2.5A RMS.
- Add 2 ON/OFF outputs driving up to 6A RMS.

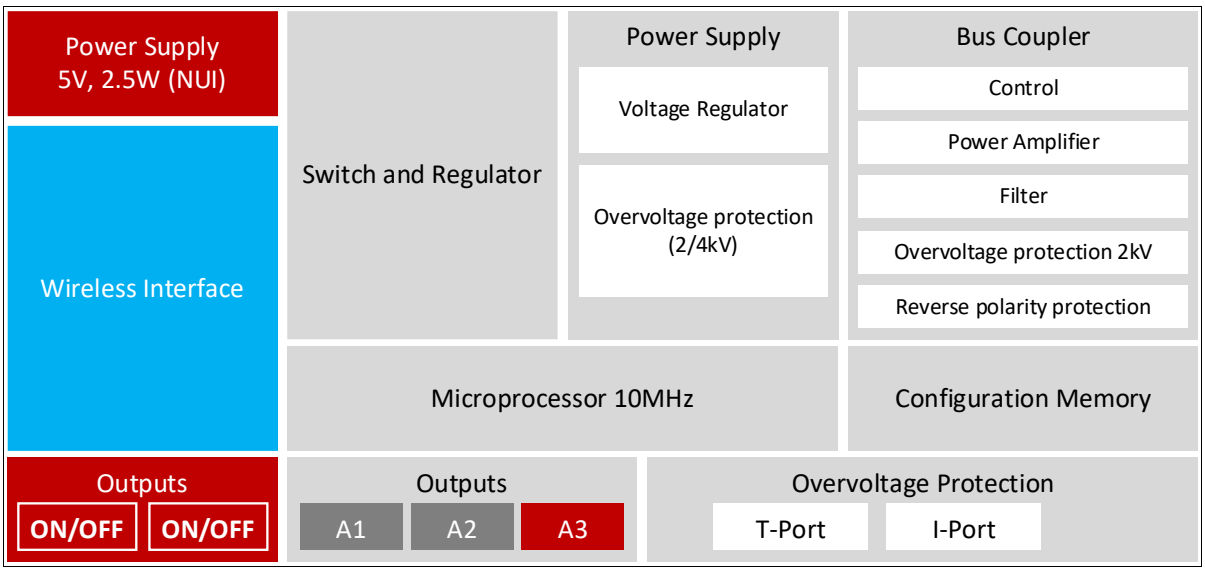

Fig. 0-9 Block diagram of internal architecture of LCN-UPU – New design Proposal.

The Power supply (5V) and the interface for wireless communication protocol will be covered in a second work as part of the digital board design upgrade. An additional required change to meet the added features is the increase of the PCB board space. There are two alternatives aligned to the conventional Mexican register box (Fig. 0-10). The selection of any of them will depend on the final design according to the PCB layout and the selected components.

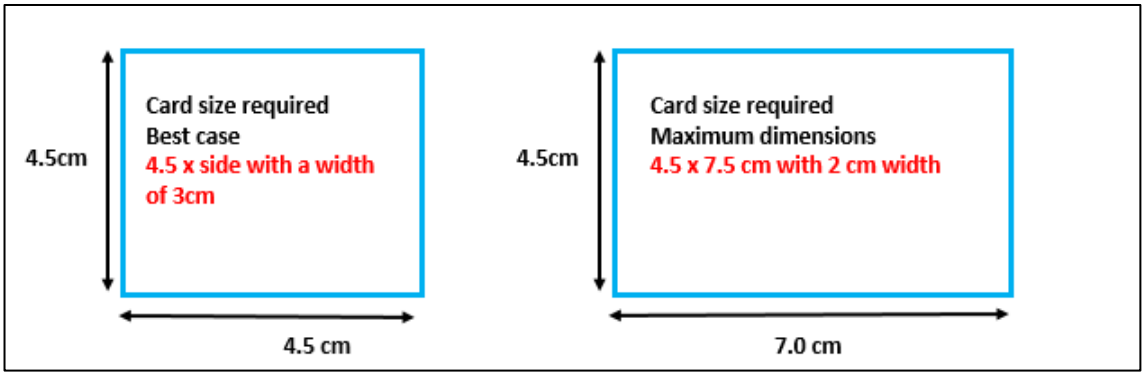

Fig. 0-10 New board size requirements.

1. MOSFET downsize

In this design upgrade the PCB saving space is relevant, therefore the MOSFET downsize was considered to meet the requirements for the power output board. The MOSFET selection was based on the electrical characteristics of the reference MOSFET design, then the thermal behavior was verified, simulated and finally a Junction Temperature (Tj) was estimated to get a reliable analysis.

1.1. Proposed Alternatives

The starting process on MOSFET selection was the electrical/thermal characteristics of the reference MOSFET device (Table 2).

Table 2 MOSFET electrical parameters (Reference design)

Supplier	**INFINEON IPD65R190C7**
Channel	N
VDS (V) max	700
$R_{dsONmax}$ (mOhm) (Vgs=10V)	168
Gate Voltage Level (V)	3,0……4,0
$R_{th\_j\text{-}c}$ (C/W, K/W) max	1.73
Id (A) (25°C) V_{gs}=10V	13
Package	DPAK
V_{gs} (V) max	± 20V
Q_{gs} (nC) max	6 (typ)
Q_{dg} (nC) max	7 (typ)
Q_g (nC) max	23 (typ)
C_{iss} (pF) max	1150 (typ)
C_{oss} (pF) max	17 (typ)
E_{AS} (mJ) max	57
E_{AR} (mJ) max	0.29
V_{sd} (V) max	0.9 (typ)
I_{sd} (A) max	-
t_{rr} (ns) max	830 (typ)
Q_{rr} (uC) max	6.5 (typ)
I_{rrm} (A) max	18 (typ)

1. MOSFET DOWNSIZE

The size of the component was the significant parameter on the searching of alternatives. Therefore, selected package into the offered market alternatives was the 5mm x 6mm MOSFET size (named differently by each supplier according to the leads' types and technology, but essentially same size devices). These packages combine the reduced volume (around 80% less) with a reduction also of internal and external parasitics coming from lead length (Fig. 1-1). [7]

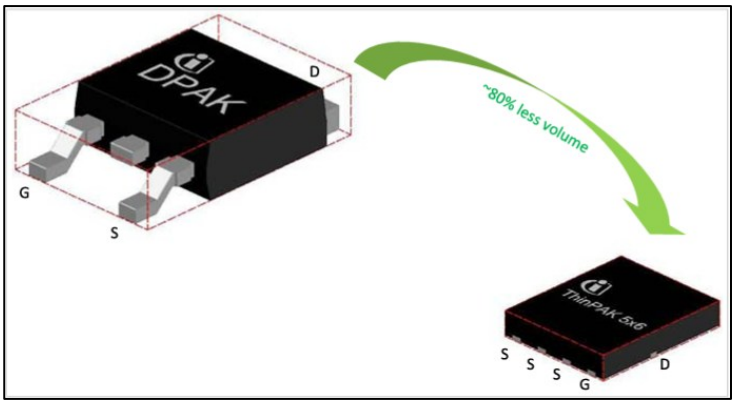

Fig. 1-1 DPAK v.s. 5x6 size MOSFET volume reduction (R. Mente, "Addressing space and efficiency in high-power applications," Power Systems Design)

Table 3 Market alternatives found with 5x6 package size & similar electrical characteristics than INFINEON - IPD65R190C7(DPAK)

Supplier	INFINEON IPLK60R360PFD7	VISHAY SiHJ240N60E	ST MICRO STL18N65M5
Channel	N	N	N
VDS (V) max	650	650	650
$R_{dsONmax}$ (mOhm) (Vgs=10V)	303	208	215
Gate Voltage Level (V)	3,5……4,5	3,0……5,0	3,0……5,0
$R_{th\_j\text{-}c}$ (C/W, K/W) max	1.7	1.4	2.2
Id (A) (25°C) V_{gs}=10V	13	12	15
Package	**ThinPAK5x6**	**PowerPAK SO-8L**	**PowerFLAT 5x6 HV**
V_{gs} (V) max	± 20V	± 30V	± 25V
Q_{gs} (nC) max	3 (typ)	4 (typ)	8 (typ)
Q_{dg} (nC) max	4.4 (typ)	6 (typ)	14 (typ)
Q_g (nC) max	12.7 (typ)	23	31 (typ)
C_{iss} (pF) max	534 (typ)	785 (typ)	1240 (typ)
C_{oss} (pF) max	12 (typ)	50 (typ)	32 (typ)
E_{AS} (mJ) max	29	81	210
E_{AR} (mJ) max	0.14	-	-
V_{sd} (V) max	1 (typ)	1.2	1.5
I_{sd} (A) max	-	12	15
t_{rr} (ns) max	90	418	290 (typ)
Q_{rr} (uC) max	0.28	4.2	4 (typ)
I_{rrm} (A) max	4.1 (typ)	18 (typ)	24 (typ)

Table 3 shows an overview of the market alternatives found with 5x6 package size. Main challenge on the MOSFET size reduction is thermal resistance potential increase due to less MOSFET size, less footprint contact means less space for thermal dissipation. These alternatives were evaluated through Worst Case Analysis (WCA) and simulated using suppliers Spice models.

1.2. Worst Case Analysis

The mathematical analysis known as Worst Case Analysis (WCA) was used to perform extreme value analysis (EVA) to predict the likelihood of extreme values in certain voltage & temperature conditions for Power dissipation. The tool used to perform this analysis was Mathcad Prime 10 (PTC Mathcad®).

The procedure to address the WCA was to model the current load behavior to calculate the Power losses (conduction & switching) and estimate the junction temperatures using thermal resistance values. A re-estimation should be necessary using thermal measurements on the original board to get more accurate thermal resistance values and T junction estimation.

The system input values are described in Fig. 1-2. Using the Mathcad capabilities all variables were set up, then it was possible to calculate many different scenarios modifying the duty cycle, load type, load values and temperature.

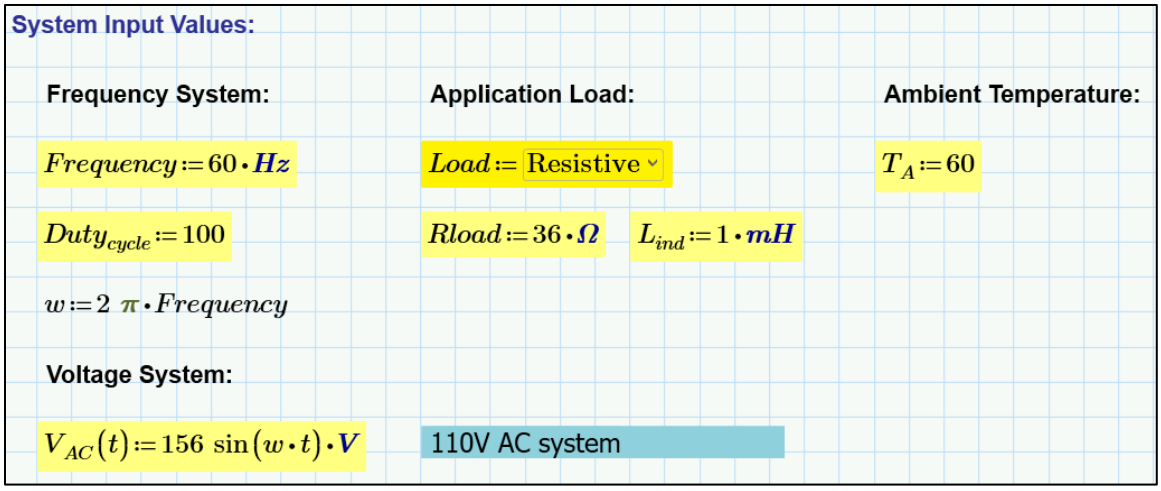

Fig. 1-2 Input variables used for Worst Case Analysis in *PTC Mathcad®*.

1.2.1 Current Load Behavior

The current load behavior was modeling considering ON and OFF scenarios. So, the current should be mapped depending on the duty cycle required, therefore following values are used in this calculation:

- Period (the inverse of frequency):

$$Period = \frac{1}{Frequency} \quad 1\text{-}1$$

- Time during ON and OFF state depending on PWM duty cycle:

$$t_{on\_pwm} = Duty_{cycle}\% \times Period \quad 1\text{-}2$$

$$t_{off\_pwm} = Period * (|100 - Duty_{cycle}\%|) \quad 1\text{-}3$$

For circuit analysis, the schematic output showed in Fig. 0-5 has been simplified and represented in Fig. 1-3.

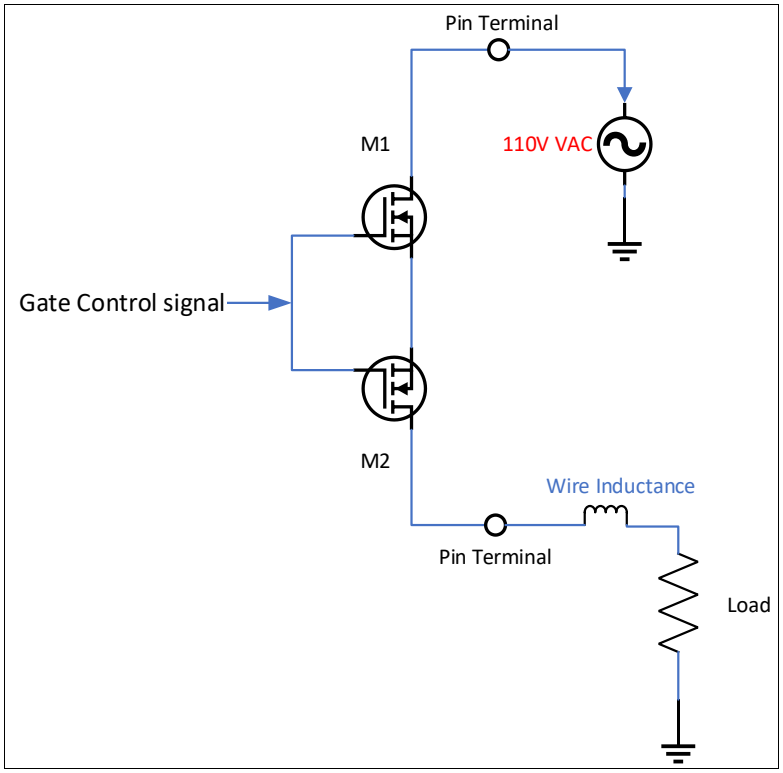

Fig. 1-3 Simplified LCN-UP output for circuit analysis.

Due to the voltage value coming from the AC source is time dependent; the current is also represented in terms of t ≥ 0s, therefore the MOSFET ON state can be described as below:

$$i_{on_{load}}(t, I_0) = \left(\frac{V_{AC}(t)}{Rload+RDson}\right) + \left(\frac{-V_{AC}(t)}{Rload+RDson}\right) * e^{-\left(\frac{Rload}{L_{ind}}\right)t} + I_0 * e^{-\left(\frac{Rload}{L_{ind}}\right)t} \quad 1\text{-}4$$

In which:

$V_{AC}(t)$	is the voltage source.
$Rload$	is the value of the load.
$RDson$	is the MOSFET resistance during ON.
L_{ind}	is the wire inductance.
I_0	is the current at t = 0s

The MOSFET OFF state is described as follows:

$$i_{off\_load}(t, I_0) = \frac{-V_{diode}}{Rload} + \left(I_0 - \frac{-V_{diode}}{Rload}\right) * e^{-\left(\frac{Rload}{L_{ind}}\right)t} \quad 1\text{-}5$$

In which:

V_{diode}	is the voltage across the MOSFET M2 body diode.

The $i_{on_{load}}$ and i_{off_load} for the t ≥ 0s should be also described depending on the duty cycle for the complete period and cycles. However, the complete code including the if statements are shown in the Appendix section.

Once the complete current waveform is modeled, voltage and current values can be calculated as below:

For V_{RMS} and I_{RMS}:

$$I_{RMS} = \sqrt{\frac{1}{Period} * \int_0^{Period} i_{load}(t)^2 dt} \quad 1\text{-}6$$

$$V_{RMS} = \sqrt{\frac{1}{Period} * \int_0^{Period} V_{AC}(t)^2 dt} \quad 1\text{-}7$$

For I_{peak} and V_{peak} when $0 = Duty_{cycle} = 100$

1. MOSFET DOWNSIZE

$$I_{peak} = i_{load}\left(\frac{Period}{4}\right) \quad 1\text{-}8$$

$$V_{peak} = V_{AC}\left(\frac{Period}{4}\right) \quad 1\text{-}9$$

For I_{peak} and V_{peak} when $0.1 \leq Duty_{cycle} \leq 99.9$

$$I_{peak} = i_{load}\left(\left(\frac{Period}{2} * Duty_{cycle}\right)\%\right) \quad 1\text{-}10$$

$$V_{peak} = V_{AC}\left(\left(\frac{Period}{2} * Duty_{cycle}\right)\%\right) \quad 1\text{-}11$$

Now the complete current waveform can be displayed, voltage and current values are shown depending on input system values. The Fig. 1-4 shows an example of I_{AC} and I_{RMS} behavior for 100% duty cycle behavior.

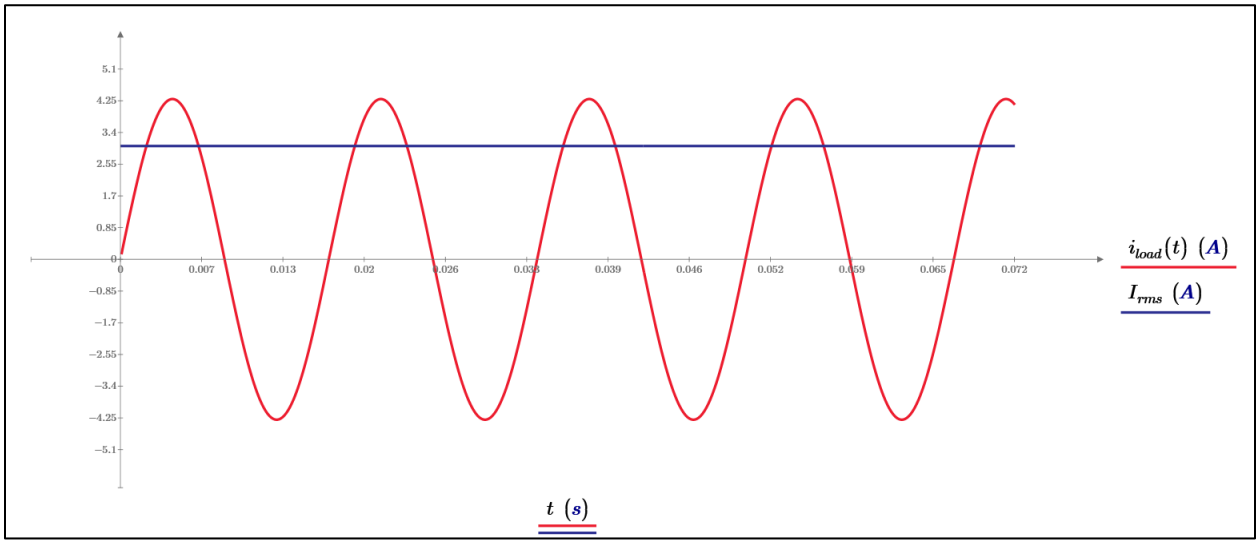

Fig. 1-4 Current load behavior for 100% duty cycle. I_{RMS} = 3.04A, V_{RMS} = 110.3V, I_{peak} = 4.3A, V_{peak} = 156V (Frequency = 60Hz, R_{load} = 36Ω)

If a different scenario needs to be evaluated, different frequency (50Hz) or different duty cycle can be modified, Fig. 1-5 shows an example of the IAC and IRMS behavior but now for 50% duty cycle.

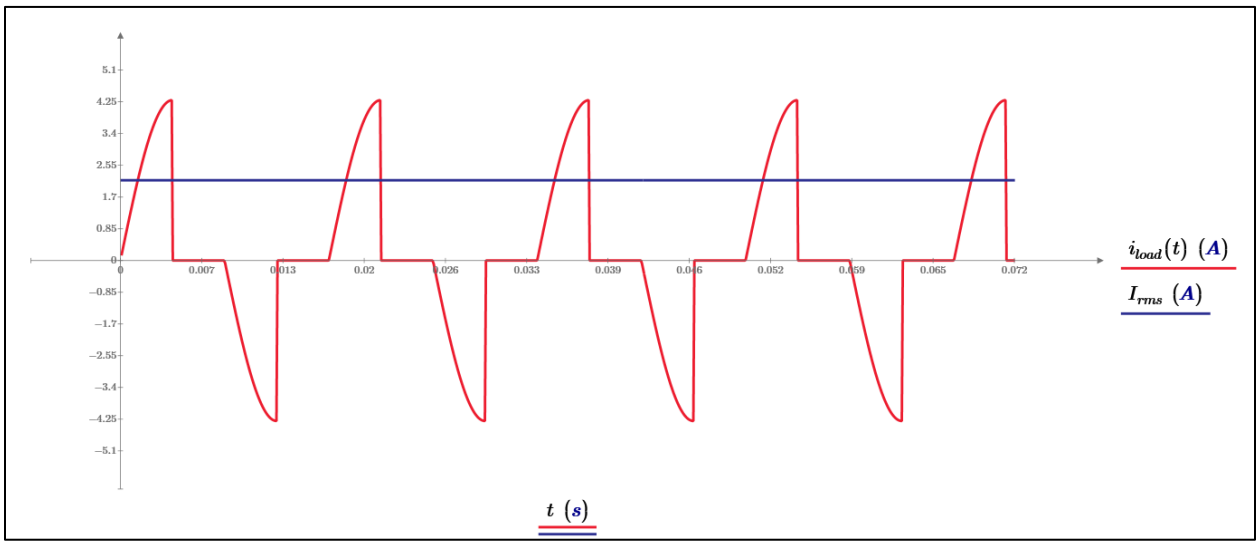

Fig. 1-5 Current load behavior for 50% duty cycle. I_{RMS} = 2.15A, V_{RMS} = 110.3V, I_{peak} = 4.3A, V_{peak} = 156V (Frequency = 60Hz, R_{load} = 36Ω)

1.2.2 Power Losses

Once the current behavior has been modeling, it will be easier to calculate the power losses on MOSFET device. Power losses can be divided in three groups:[8]

- Conduction losses P_{cond}
- Switching losses P_{switch}
- Blocking (leakage) losses P_{block}, normally neglected

Therefore:

$$P_{total} = P_{cond} + P_{switch} + P_{block} \approx P_{cond} + P_{switch} \quad 1\text{-}12$$

Conduction Losses

In our analysis, conduction losses mean the power dissipation when the MOSFET is in ON state, but first we should consider how the temperature may affect the MOSFET device. This can be estimated using the MOSFET ON resistance datasheet plot ($R_{DS(on)}$) versus junction temperature (Tj). In some datasheets a temperature coefficient parameter (α) is used to describe the relationship between them, this coefficient mostly has a positive value in MOSFET for normal operating conditions.[9]

The formula is described below:

$$R_{DS(on)} = R_{DS(on\_25C)} * \left(1 + \frac{\propto}{100}\right)^{Tj-25℃} \quad 1\text{-}13$$

In which:

$R_{DS(on\_25C)}$	is the MOSFET drain-source resistance at 25°C.
α	is the temperature coefficient.
T_j	is the MOSFET junction temperature.

Using this formula, it is possible to estimate what would be the ($R_{DS(on)}$) value at different temperatures.

The conduction losses now can be estimated in this way:

$$P_{cond} = R_{DS(on)} * \frac{1}{Period} * \int_0^{t_{on\_pwm}} i_{load}(t)^2 dt \quad 1\text{-}14$$

In which:

$R_{DS(on)}$	is the MOSFET drain-source resistance.
t_{on_pwm}	is the MOSFET ON state time.

Switching Losses

In this analysis, switching losses estimation has to do with the power dissipation in the moment of ON/OFF transition and vice versa. For this, the MOSFET switch ON and OFF times are needed and can be estimated as below:

For MOSFET switch ON time:

$$T_{swON} = \frac{Q_{gs}}{GCC} \quad 1\text{-}15$$

In which:

Q_{gs}	is the MOSFET gate-source charge value (from datasheet).
GCC	is the Gate Charge Current value from gate driver CD4093.

For MOSFET switch OFF time:

$$T_{swOFF} = \frac{Q_{gtot} - Q_{gs} - Q_{gd}}{GCC} \quad 1\text{-}16$$

In which:

Q_{gtot}	is the MOSFET total gate charge value (from datasheet)
Q_{gs}	is the MOSFET gate-source charge value (from datasheet).
Q_{gd}	is the MOSFET gate-drain charge value (from datasheet)
GCC	is the Gate Charge Current value from gate driver CD4093

The missing value on this calculation is the GCC, this value was obtained from the NAND gate CD4093 (Texas Instrument) datasheet used in the original design, and it is an estimation of Output low (sink) and high (source) currents (I_{OL} and I_{OH} respectively) at typical conditions. Given these switching times, the switching losses can be estimated in two scenarios:

When $0.1 \leq Duty_{cycle} \leq 99.9$

$$P_{switch} = \frac{1}{2} * (T_{swON} + T_{swOFF}) * (V_{peak} + V_{diode}) * I_{RMS} * Frequency \quad 1\text{-}17$$

1.2.3 Thermal Behavior

To obtain an estimation of the junction temperature of MOSFET and PCB temperatures the thermal model of the single MOSFET shown in Fig. 1-6 is used.

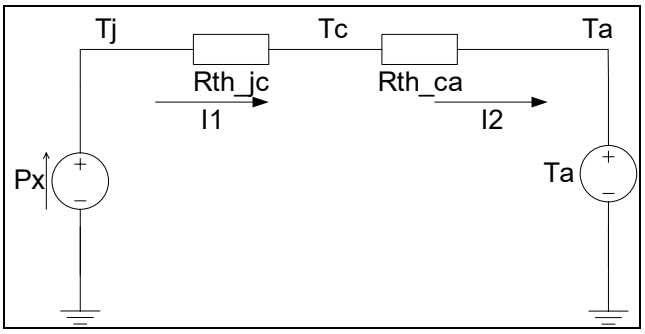

Fig. 1-6 Single MOSFET thermal model

The equation for MOSFEET junction temperature:

$$T_j = P_{total} * R_{th_{jc}} + P_{total} * R_{th_{ca}} + Ta \quad 1\text{-}18$$

In which:

P_{total} is the total power dissipation obtained from equation:

$$P_{total} = P_{cond} + P_{switch} + P_{block} \approx P_{cond} + P_{switch} \quad 1\text{-}12$$

R_{th_jc} is the MOSFET thermal resistance junction to case (from datasheet).

R_{th_ca} is the MOSFET thermal resistance case to ambient (from datasheet).

Ta is the ambient temperature.

The equation to estimate the PCB temperature underneath MOSFET baseplate:

$$T_{PCB} = P_{total} * R_{th_{ca}} + Ta \quad 1\text{-}19$$

1.2.4 Summary

Using the input values in Fig. 1-2 the worst-case analysis calculation (power losses and Tj estimation) now can be performed. Two scenarios are presented, the first one (Fig. 1-7) with 50% duty cycle (to visualize the switching and conduction losses) and the second one (Fig. 1-8) with 100% duty cycle (only conduction losses).

LOAD CONDITION					
VRMS (V)	110.31	Frequency (hz)	60	Duty (%)	50
IRMS (A)	2.15	IPEAK (A)	4.30	VPEAK (V)	156.00

$T_A = 60$

MOSFET RESULTS												
Supplier / Package	Infineon - IPD65R190C7 DPAK			Infineon - IPLK60R360PFD7 ThinPAK 5x6			Vishay - SiHJ240N60E PowerPAK SO-8L			ST Micro - STL18N65M5 PowerFLAT 5x6 HV		
Parameter	min	typ	max	min	typ	max	min	typ	max	min	typ	max
Slew-Rate ON (V/us)	47.691	95.383	143.074	75.873	151.745	227.618	55.640	111.280	166.920	23.846	47.691	71.537
Slew-Rate OFF (V/us)	47.691	95.383	143.074	75.873	151.745	227.618	55.640	111.280	166.920	23.846	47.691	71.537
Conduction Losses (W)	0.462	0.462	0.462	0.833	0.833	0.833	0.572	0.572	0.572	0.591	0.591	0.591
Switching Losses (W)	0.022	0.033	0.066	0.014	0.021	0.042	0.019	0.028	0.057	0.044	0.066	0.132
Total Losess (W)	0.484	0.495	0.528	0.847	0.854	0.874	0.591	0.600	0.628	0.635	0.657	0.723
Max. Tamb (°C)	60.000			60.000			60.000			60.000		
Max. Tsolder (°C)	60.913			61.487			60.880			61.591		
Max. Tjunction (°C)	93.643			131.443			111.153			119.445		

Fig. 1-7 Worst case analysis for MOSFET proposed alternatives (50% duty cycle, R_{load} = 36Ω).

LOAD CONDITION					
VRMS (V)	110.31	Frequency (hz)	60	Duty (%)	100
IRMS (A)	3.04	IPEAK (A)	4.30	VPEAK (V)	156.00

$T_A = 60$

MOSFET RESULTS												
Supplier Package	Infineon - IPD65R190C7 DPAK			Infineon - IPLK60R360PFD7 ThinPAK 5x6			Vishay - SiHJ240N60E PowerPAK SO-8L			ST Micro - STL18N65M5 PowerFLAT 5x6 HV		
Parameter	min	typ	max	min	typ	max	min	typ	max	min	typ	max
Slew-Rate ON (V/us)	47.691	95.383	143.074	75.873	151.745	227.618	55.640	111.280	166.920	23.846	47.691	71.537
Slew-Rate OFF (V/us)	47.691	95.383	143.074	75.873	151.745	227.618	55.640	111.280	166.920	23.846	47.691	71.537
Conduction Losses (W)	1.847	1.847	1.847	3.332	3.332	3.332	2.287	2.287	2.287	2.364	2.364	2.364
Switching Losses (W)	0.000	0.000	0.000	0.000	0.000	0.000	0.000	0.000	0.000	0.000	0.000	0.000
Total Losess (W)	1.847	1.847	1.847	3.332	3.332	3.332	2.287	2.287	2.287	2.364	2.364	2.364
Max. Tamb (°C)	60.000			60.000			60.000			60.000		
Max. Tsolder (°C)	63.196			65.664			63.202			65.201		
Max. Tjunction (°C)	177.726			332.197			246.168			254.325		

Fig. 1-8 Worst case analysis for MOSFET proposed alternatives (100% duty cycle, R_{load} = 36Ω).

Due the Tj estimated (~178°C) for Infineon – IPD65R190C7 looks higher than the maximum Tj allowed (150°C), we can assume the value of Rth_{CA} should be less than 62 K/W in the actual design (DPAK), otherwise the excess of power dissipation would damage the MOSFET. A new Rth_{CA} estimation would be required for DPAK and 5x6 packages to get a reliable Tj estimation.

1.3. Thermal measurements for MOSFET Tj re-estimation.

To estimate the MOSFET thermal performance, a method described by supplier Vishay on the Application Note AN819 was applied directly on the PCB. [10] The main idea behind this procedure is to dissipate a known power value though the MOSFET and measuring the temperature increase this causes in the junction. This provide the data required to calculate the junction to ambient thermal resistance (°C/W).

First, a characterization of the body diode was required to measure the MOSFET junction temperature. Using the MOSFET mounted on the PCB (DPAK Infineon - IPD65R190C7) the gate is connected to the source to avoid MOSFET turning on. Then a 10mA current is passed through the body diode and the forward voltage (V_F) is measured at room and high temperature (25°C and 100°C respectively). The diode temperature coefficient is calculated using the following equation:

1. MOSFET DOWNSIZE

$$T_C = \frac{V_F@100°C - V_F@25°C}{100°C - 25°C} = \frac{359mV - 537mV}{100°C - 25°C} = -2.37mV/°C \quad 1\text{-}20$$

Where:

$V_F@100°C$	is the body diode forward voltage at 100°C.
$V_F@25°C$	is the body diode forward voltage at 25°C.

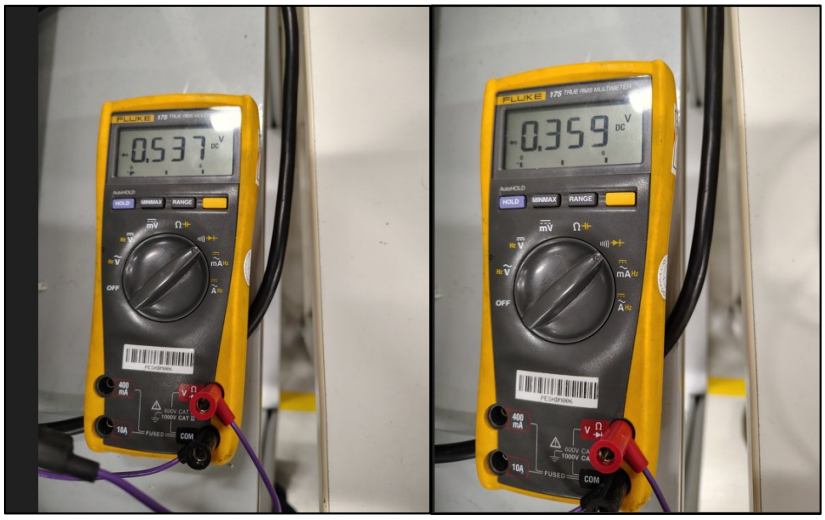

Fig. 1-9 Body diode forward voltage measurement at 25°C (left) and 100°C (right).

Now the same board is connected as the setup showed in Fig. 1-10, two current sources are connected between the drain and source MOSFET pins. One current is configured as constant current source (1.5A or 3A) and its used as "heating current", the other power supply is used as sensing current (10mA). Both power supplies are connected in parallel and separated by a switch.

The procedure to measure the temperature rise and then calculate thermal resistance is:

1. Close the switch, the current through the body diode will dissipate approximately 1W after equilibrium is reached (equilibrium means V_F is stabilized).

2. Power is estimated ($P_D = V_F \times I_F$)

3. Open the switch, the current should drop to 10mA (second current source). The V_F should be measured immediately using a digital oscilloscope.

4. ΔV_F is calculated (negative value)

5. ΔT_J is calculated using ΔV_F / T_C

6. Finally, R_{thJA} is calculated using ΔT_J / P_D

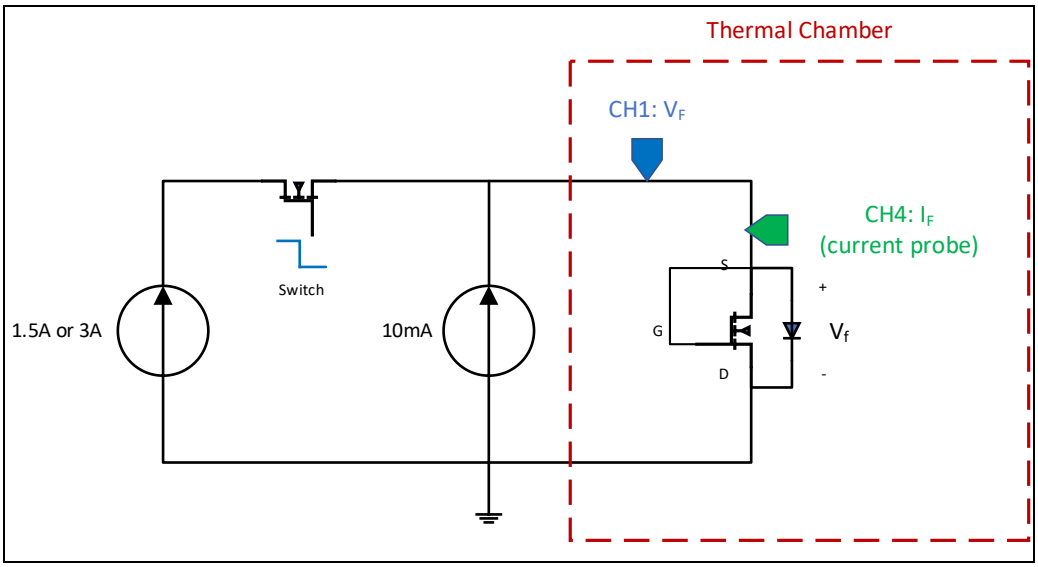

Fig. 1-10 Tcase measurement setup using current sources and digital oscilloscope

Following the described steps, the calculation of the P_D is:

$$P_D = V_F \times I_F = 0.732V \times 1.512A = 1.1W \quad (1\text{-}21)$$

ΔV_F calculation is:

$$\Delta V_F = 511mV - 562.3mV = -50.9mV \quad (1\text{-}22)$$

ΔT_J calculation is:

$$\Delta T_J = \frac{\Delta V_F}{T_C} = \frac{-50.9mV}{-2.37mV/°C} = 21.48°C \quad (1\text{-}23)$$

Finally, R_{thJA} calculation is:

$$R_{thJA} = \frac{\Delta T_J}{P_D} = \frac{21.48°C}{1.1W} = 19.5° \frac{C}{W} = 19.5 \frac{K}{W} \quad (1\text{-}24)$$

1. MOSFET DOWNSIZE

Even though the R_{thJA} value has been estimated, we can add a 30% error margin considering these measurements were not performed inside the plastic housing, then our final value for DPAK Infineon - IPD65R190C7 MOSFET is:

$$R_{thJA\_F} = R_{thJA} + 30\% = 19.5\frac{K}{W} + 30\% = 25.3\frac{K}{W} \quad 1\text{-}25$$

This value results in 140% less than the used in our worst case first estimation (using datasheet minimal footprint values). The main idea is to keep the same copper area for new MOSFETs therefore using this relation, we can also estimate a new value for 5x6 packages. Table 4 shows this estimation.

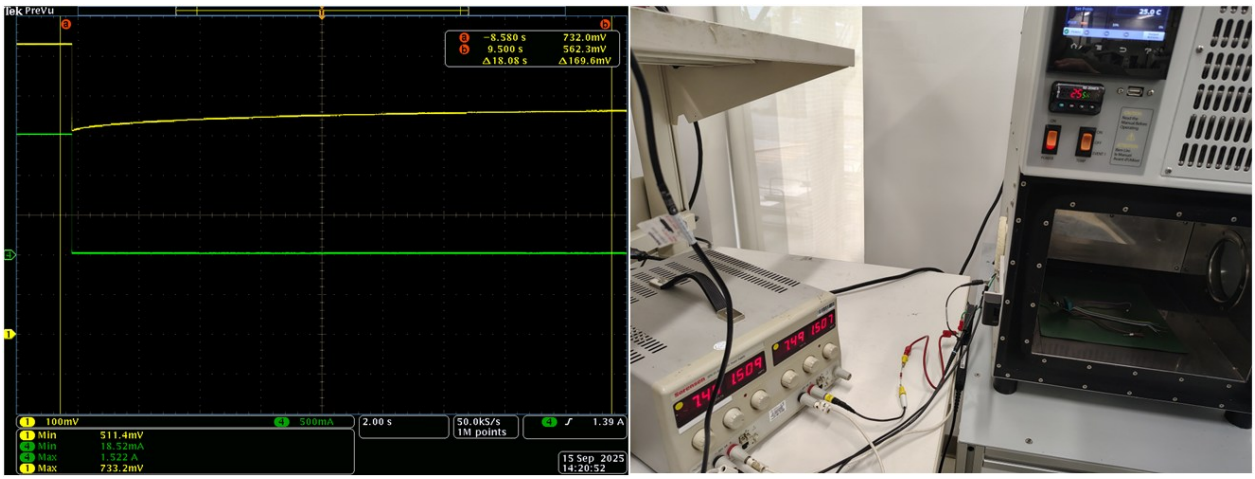

Fig. 1-11 Current drop between heating current (~1.5A) and sensing current (10mA) and Tcase measurement setup.

Table 4 Final R_{thCA} after Tj re-estimation.

Package	Minimal footprint R_{thCA} on datasheet	Measured R_{thCA} value	Error margin	Final R_{thCA} value after Tj re-estimation
DPAK	62 K/W	19.5 K/W	30%	25.3 K/W
5x6	80 K/W	-		32.6 K/W

Finally, the new estimated values for DPAK and 5x6 packages are used in the worst case calculations, using again the two scenarios, with 50% duty cycle to visualize the switching and conduction losses (Fig. 1-12) and the second one with 100% duty cycle for only conduction losses

(Fig. 1-13). Under this new calculation, only one MOSFET (INFINEON IPLK60R360PFD7) is not fulfilling the Tj maximum rating (150°C), hence this option may be discarded in the design upgrade.

LOAD CONDITION						
VRMS (V)	110.31	Frequency (hz)	60	Duty (%)	50	$T_A = 60$
IRMS (A)	2.15	IPEAK (A)	4.30	VPEAK (V)	156.00	

MOSFET RESULTS												
Supplier Package	Infineon - IPD65R190C7 DPAK			Infineon - IPLK60R360PFD7 ThinPAK 5x6			Vishay - SiHJ240N60E PowerPAK SO-8L			ST Micro - STL18N65M5 PowerFLAT 5x6 HV		
Parameter	min	typ	max	min	typ	max	min	typ	max	min	typ	max
Slew-Rate ON (V/us)	47.691	95.383	143.074	75.873	151.745	227.618	55.640	111.280	166.920	23.846	47.691	71.537
Slew-Rate OFF (V/us)	47.691	95.383	143.074	75.873	151.745	227.618	55.640	111.280	166.920	23.846	47.691	71.537
Conduction Losses (W)	0.462	0.462	0.462	0.833	0.833	0.833	0.572	0.572	0.572	0.591	0.591	0.591
Switching Losses (W)	0.022	0.033	0.066	0.014	0.021	0.042	0.019	0.028	0.057	0.044	0.066	0.132
Total Losess (W)	0.484	0.495	0.528	0.847	0.854	0.874	0.591	0.600	0.628	0.635	0.657	0.723
Max. Tamb (°C)	60.000			60.000			60.000			60.000		
Max. Tsolder (°C)	60.913			61.487			60.880			61.591		
Max. Tjunction (°C)	74.269			89.994			81.366			85.167		

Fig. 1-12 Worst case analysis for MOSFET proposed alternatives (50% duty cycle, R_{load} = 36Ω) with final R_{thCA} after Tj re-estimation.

LOAD CONDITION						
VRMS (V)	110.31	Frequency (hz)	60	Duty (%)	100	$T_A = 60$
IRMS (A)	3.04	IPEAK (A)	4.30	VPEAK (V)	156.00	

MOSFET RESULTS												
Supplier Package	Infineon - IPD65R190C7 DPAK			Infineon - IPLK60R360PFD7 ThinPAK 5x6			Vishay - SiHJ240N60E PowerPAK SO-8L			ST Micro - STL18N65M5 PowerFLAT 5x6 HV		
Parameter	min	typ	max	min	typ	max	min	typ	max	min	typ	max
Slew-Rate ON (V/us)	47.691	95.383	143.074	75.873	151.745	227.618	55.640	111.280	166.920	23.846	47.691	71.537
Slew-Rate OFF (V/us)	47.691	95.383	143.074	75.873	151.745	227.618	55.640	111.280	166.920	23.846	47.691	71.537
Conduction Losses (W)	1.847	1.847	1.847	3.332	3.332	3.332	2.287	2.287	2.287	2.364	2.364	2.364
Switching Losses (W)	0.000	0.000	0.000	0.000	0.000	0.000	0.000	0.000	0.000	0.000	0.000	0.000
Total Losess (W)	1.847	1.847	1.847	3.332	3.332	3.332	2.287	2.287	2.287	2.364	2.364	2.364
Max. Tamb (°C)	60.000			60.000			60.000			60.000		
Max. Tsolder (°C)	63.196			65.664			63.202			65.201		
Max. Tjunction (°C)	109.931			174.276			137.761			142.269		

Fig. 1-13 Worst case analysis for MOSFET proposed alternatives (100% duty cycle, R_{load} = 36Ω) with final R_{thCA} after Tj re-estimation.

1.4. Electrical Simulation

In parallel, the power stage circuit portion was electrically simulated to validate the circuit behavior and compare it to WCA results. In this simulation, only one leg (one output) was

considered. The switching behavior was adapted to avoid issues with ground references (e.g. NAND gates spice model) and replaced by a couple of switches and sources. This array (Fig. 1-14) allowed us to modify the required duty cycle by simply modifying the pulse power supply parameters. Both scenarios, 50% (Fig. 1-15) and 100% (Fig. 1-16) were simulated for all the MOSFETs suppliers, a summary of the simulation result is shown in Table 5.

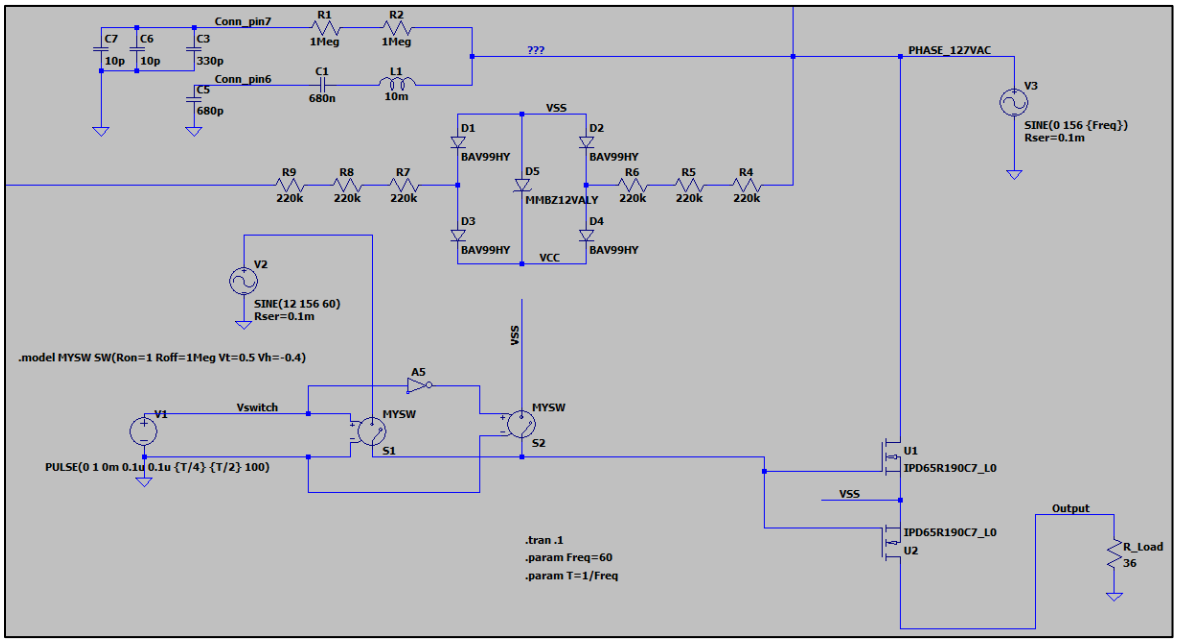

Fig. 1-14 Electrical simulation for MOSFET switching behavior for one output.

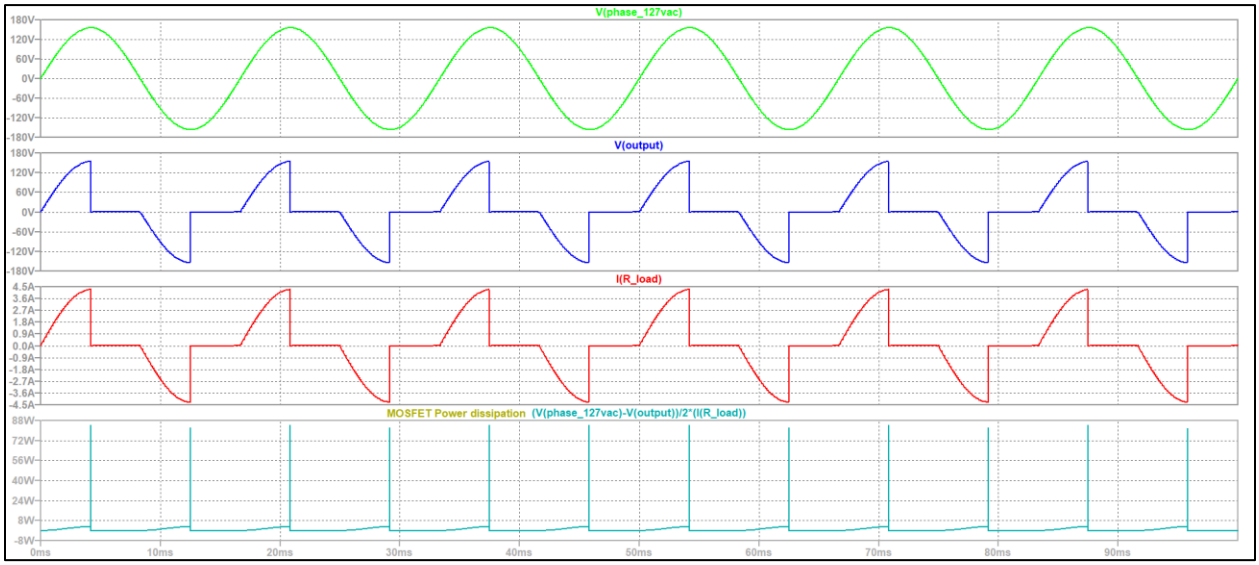

Fig. 1-15 Electrical waveforms for Input/Output voltage, current load and MOSFET power dissipation (50% duty cycle, R_{load} = 36Ω)

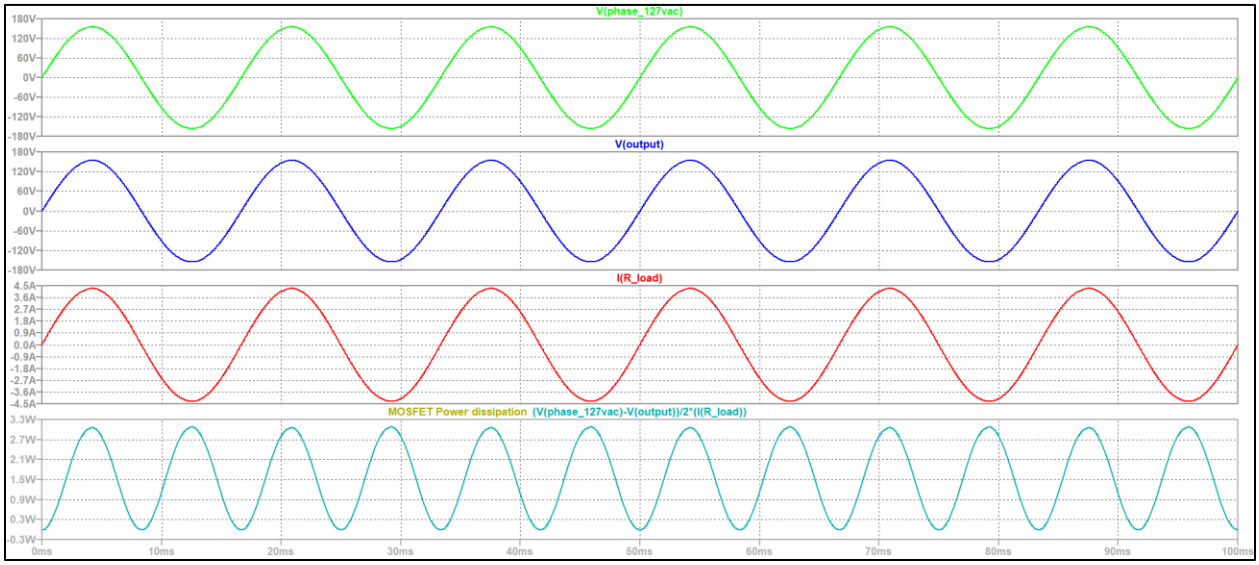

Fig. 1-16 Electrical waveforms for Input/Output voltage, current load and MOSFET power dissipation (100% duty cycle, R_{load} = 36Ω)

Table 5 Summary for comparison between WCA and simulation results.

50% DC		WCA	Simulation
	V_{RMS}	110.31 V	110.31 V
	I_{RMS}	2.15 A	2.14 A
	I_{PEAK}	4.30 A	4.28 A

100% DC		WCA	Simulation
	V_{RMS}	110.3 V	110.31 V
	I_{RMS}	3.04 A	3.03 A
	I_{PEAK}	4.30 A	4.28 A

	INFINEON IPD65R190C7		**INFINEON IPLK60R360PFD7**		**VISHAY SiHJ240N60E**		**ST MICRO STL18N65M5**	
	WCA	Simulation	WCA	Simulation	WCA	Simulation	WCA	Simulation
Total Losses 50% DC	0.528 W	0.785 W	0.874 W	1.246 W	0.628 W	No SPICE model available	0.723 W	0.998 W
Total Losses 100% DC	1.847 W	1.563 W	3.332 W	2.459 W	2.287 W		2.364 W	1.822 W

The differences observed in total losses are related to the method used for WCA (extreme value analysis) and temperature. In general, the calculated power dissipation values are not far from the simulated ones using the supplier electrical model. This information increases the level of confidence to continue on the design upgrade process.

2. Relay selection

The relay selection was based on the LCN-R10 module design also from the company Issendorff KG. The relay HF49FD from Hongfa Technology Co. can operate at maximum 5A (250VAC). The specified value for our loads is 6A, therefore in the following sections an estimation is carried out to verify the meeting requirements.

Table 6 HF49FD contact data

(extracted from HF49FD spec sheet from Hongfa Technology Co.)

CONTACT DATA	
Contact arrangement	1A
Contact Resistance (at 1A 6VDC)	No gold plated: 100mΩ max. Gold plated: 50mΩ max.
Contact material	$AgSnO_2$, AgNi
Contact rating (Res. Load)	5A 250VAC/30VDC
Max. switching voltage	250VAC / 125VDC(at 0.3A)
Max. switching current	5A
Max. switching power	1250VA / 150W
Min. contact load	No gold plated: 5VDC 10mA Gold plated: 5VDC 1mA

2.1. Relay circuit protection

As well as the MOSFET outputs, the relay contact should be protected in case of excessive current or voltage during operation. The expected load for the two 6A ON/OFF loads are motors therefore, protection must be considered accordingly an inductive load behavior. Main issue driving inductive loads is the voltage spike created when the output is switched off, a surge suppressor of voltage/current is recommended to prevent arcing between the contacts and increase the lifetime of the Relay.

For AC motor loads the most common surge suppressors are the RC array (snubber) and the Metal Oxide Varistor (MOV) [11], both are placed in parallel with the load. The RC snubber is a network which consist in a capacitor and resistor in series, it is used as arc and inrush

suppressor. When the relay is switched off an arc could be created across the contacts, then using an RC snubber, contacts voltage goes through the snubber capacitor, which gets charged faster than the mechanical motion of the contacts disconnecting. In the same way, when the relay is switched on, an inrush current could be produced by the power supply and the charged capacitor, thus, the snubber resistor shall absorb this current and act as a current limiter. In other words, the RC snubber will limit a maximum dv/dt across the relay element. [12]

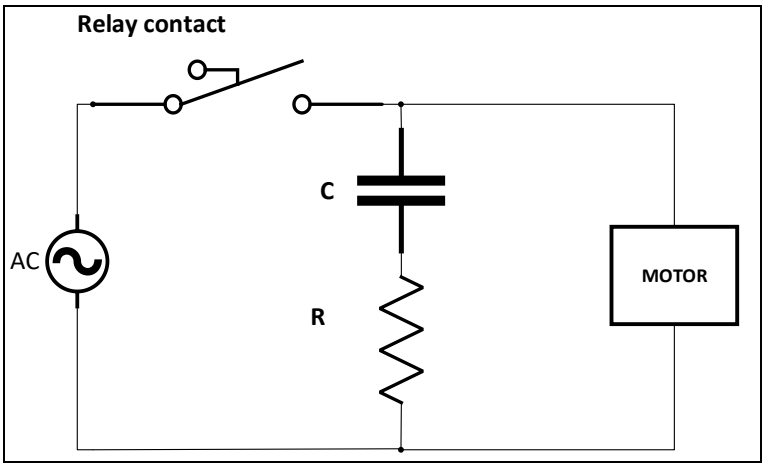

Fig. 2-1 Inductive load suppression using RC snubber.

The MOV, or simply Varistor, is a voltage dependent resistor. This resistance is high when the operating voltage is below and it's low when this voltage is above. Therefore, this component is also used to limit the voltage and di/dt across the relay contacts during switch off stage. [13]

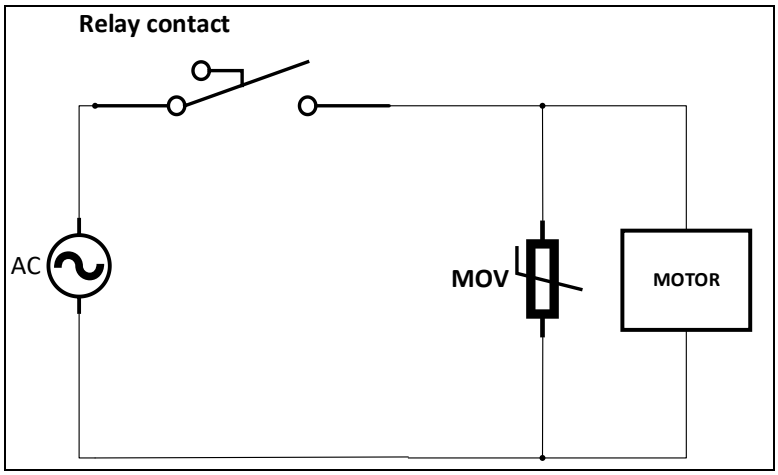

Fig. 2-2 Inductive load suppression using MOV.

The MOV has some limitations, one is this component can only absorb certain number of surges, and they are not suitable for high frequency signals. [14] In this design, a combined approach of both solutions is used. The RC snubber is more efficient for limiting the voltage across the relay contact when during the switch off/on process, while MOV is more efficient in limiting voltage spikes caused by power grid fluctuations.

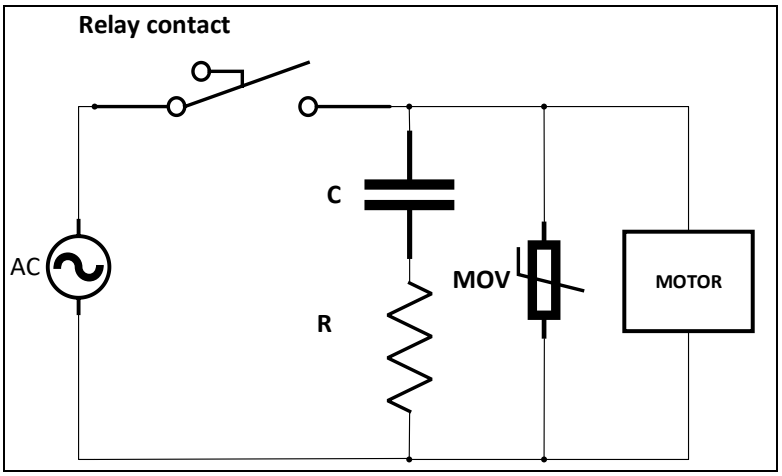

Fig. 2-3 Inductive load suppression using MOV and RC snubber.

2.1.1 RC Snubber and MOV value estimation

In different relay supplier guidelines, it is mentioned that the RC snubber selection is an empirical process and should be refined experimentally. [15] As rule of thumb, it was taken 0.1uF per 1 Ampere for the capacitor and 1Ω per 1V for the resistor. Therefore, for $120V_{AC}$ and 6A, the values should be 120Ω and 0.6uF respectively. Given these values, a near approximation was found with supplier Knowles for 0.5uF and 100Ω:

- Part Number / Supplier: 504M02QA100 / Cornell Dubilier Knowles

For the MOV component selection, the recommended cutoff voltage selection is based on $Vc = \sqrt{2} * 120V_{AC}$, therefore the value should be near to 169V, however it is also mentioned that the effectiveness could be reduced if Vc is set too high. [11] Based on before statement a near approximation selected was Vc=150V with supplier TDK:

- Part number / Supplier: CU3225K150G2 / TDK Electronics

2.2. Relay Power Analysis

From datasheet information, the analysis of the relay is focused on contact and coil losses. For contact losses we simply verify the maximum switching power allowed (1200VA), this value is deducted from the maximum contact rating:

$$P_{AC} = I_{AC} * V_{AC} = 5A * 250V = 1200VA \quad 2\text{-}1$$

For our case the maximum VAC expected approximately 180V resulted from:

$$V_{AC} = V_{RMS} * \sqrt{2} = 127V * \sqrt{2} = 179.6V \quad 2\text{-}2$$

Therefore, if the requirement is to drive maximum 6A, the maximum contact power would be less than the maximum contact rating ($P_{AC} = I_{AC} * V_{AC} = 5A * 250V$=$1200VA$ 2-1):

$$P_{AC} = 6A * 180V = 1080VA \quad 2\text{-}3$$

For contact losses we selected the nominal voltage of 12V, therefore according to the specification the coil resistance would be 1200Ω ± 10%, here the min and max current would be:

$$Icoil_{min} = \frac{12V}{1200\Omega*(1+10\%)} = 9.1mA \quad 2\text{-}4$$

$$Icoil_{max} = \frac{12V}{1200\Omega*(1-10\%)} = 11.1mA \quad 2\text{-}5$$

The max power dissipation in coil considering a stable 12V supply is:

$$Pcoil_{max} = V * Icoil_{max} = 12V * 11.1mA = 133.3mW \quad 2\text{-}6$$

Even though this value is higher than the 120mW indicated in the datasheet, this is an approximated value, therefore we consider part of the variation expected during relay operation.

3. Bill of Material (BOM)

Once all interfaces were defined, the list of required components (Bill of Materials) for the upgraded power stage board is shown in Table 7. The list of components is considering 3 PWM outputs 2.5A RMS and 2 new ON/OFF output 6A RMS, therefore a total of 5 power outputs will be populated in this board.

Table 7 Bill of material for Power stage board for design upgrade

Qty	Value	Part Function	Package	Supplier name	Supplier part number
5	47	Resistor	0603	Vishay	CRCW060347R0JNEAC
5	100k	Resistor	0603	Vishay	CRCW0603100KJNEAC
1	10mH	Inductor	Axial	TT Electronics	HM51-103KLF
2	1M	Resistor	1206	Vishay	CRCW12061M00JNEAC
5	1n	Capacitor	0603	Samsung Electro-Mech	CL10B102KC8NNWC
30	220k	Resistor	1206	TE Connectivity	CRGP1206F220K
5	220k	Resistor	0603	Vishay	CRCW0603220KFKEAC
5	4.7u	Capacitor	1206	Murata Electronics	GRM31CZ72A475KE11L
1	47k	NTC	0805	Ametherm	SM08503395
2	504M02QA100	Snubber	Radial	Knowles	504M02QA100
5	56n	Capacitor	0603	Kemet	C0603C563K1RACTU
1	680n	Capacitor	Radial	Kemet	F461DB684J250
1	680p	Capacitor	0603	Kyocera AVX	06031C681KAT4A
10	BAV99	Diode	SOT23	Nexperia	BAV99
5	CD4093B	NAND gate	TSSOP14	Texas Instrument	CD4093BPWR
5	CU3225K150G2	Varistor	3225	TDK	B72650M0151K072
2	HF49FD	Relay		Hongfa	HF49FD/012-1H12TB
5	HMHA2801	Optocoupler	MPF4	Onsemi	FODM217D
5	MM3Z12	Diode	SOD-323F	Diotec Semiconductor	MM3Z12
1	PCB 4Layers	PCB	70mm x 45mm x 1mm		
6	STL18N65M5	Mosfet	PowerFLAT 5x6	ST Micro	STL18N65M5
6	TPSMB12CA-VR	TVS bidirectional	SMB	Littlefuse	TPSMB12CA-VR
6	Cable	Cable connector			

3.1. Cost evaluation: old vs. new

Even though the cost analysis compares the old and new design with 2 and 5 respectively, this exercise was performed to highlight the advantage of the presented solution. It is evident that adding new outputs (components) will impact on the cost of the new solution (Table 8) however,

a profitable scenario is achieved when this comparison is taken to system level (Table 9). A complete cost analysis including logic and power board will be presented in another work.

Table 8 Cost Analysis per power board, old vs. new design

COST COMPARISON FOR POWER BOARD		
	Old Power Board 2 PWM 2.5A	**New Power Board** 3 PWM 2.5A 2 ON/OFF 6A
* Price (USD)	$ 17.12	$ 65.40

** Quoted prices per 100 pieces from Mouser, Digikey, PCB Way and TME Electronic components on Nov 24th, 2025.*

Table 9 Cost Analysis per solution, required modules per solution using old and new design.

COST COMPARISON FOR POWER BOARD (PER SOLUTION)					
Old Design	Required modules	* Price (USD)	New Design	Required modules	* Price (USD)
2 PWM 2.5A	2	$ 34.24	3 PWM 2.5A 2 ON/OFF 6A	1	$ 65.40
2 ON/OFF 6A	1	$ 39.90			
TOTAL	**3**	**$ 74.14**		**1**	**$ 65.40**

** Quoted prices per 100 pieces from Mouser, Digikey, PCB Way and TME Electronic components on Nov 24th, 2025.*

3.2. PCB Layer increase

A significant improvement in thermal performance is obtained when the number of PCB layers are increased. [16] In this design upgrade, an increase of 2 additional layers is proposed, this change would impact the power stages PCB board cost in near to 135% however, as is shown in Table 9 the expected benefit would be obtained at whole solution implementation.

4. New design

The final process in this work is the preparation of the new design schematic as well as the preliminary layout & component placement.

4.1. Schematic Development

The Fig. 4-1 shows the power supply section and topology of one PWM output 2.5A RMS, same topology is shared by output 2 and 3.

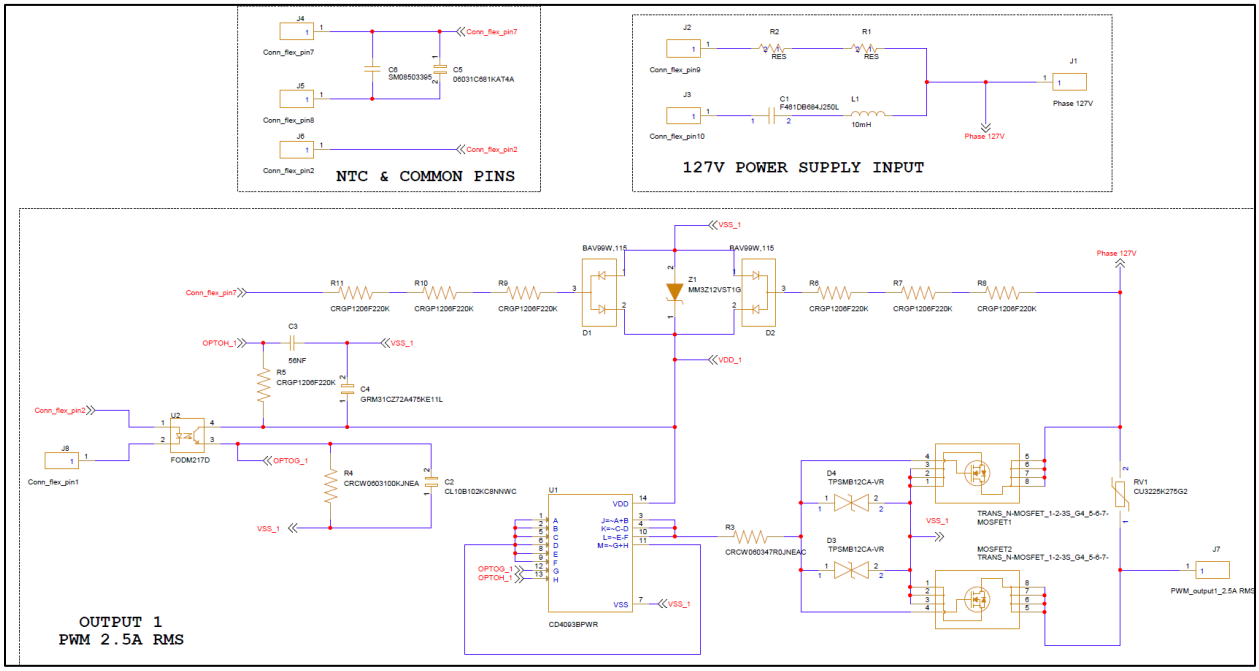

Fig. 4-1 Schematic view for PWM outputs 2.5A RMS (Outputs 1 to 3).

The Fig. 4-1 shows the topology of the new ON/OFF output 6A RMS, same topology is shared by output 4 and 5.

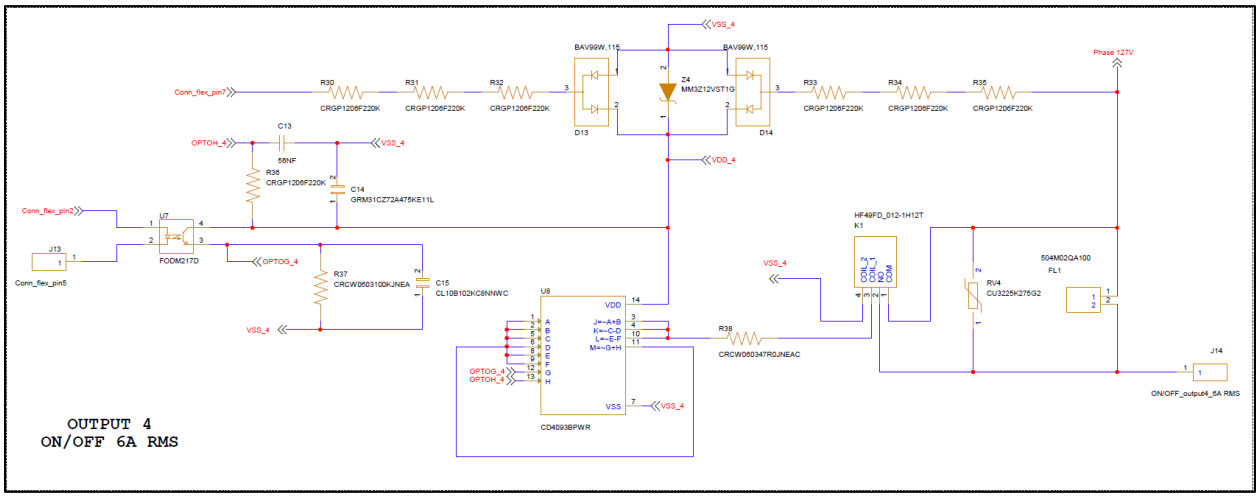

Fig. 4-2 Schematic view for ON/OFF outputs 6A RMS (Outputs 4 and 5).

4.2. PCB Layout

The preliminary PCB layout is shown in Fig. 4-3 and Fig. 4-4. This board consider the extended size to cover the 5 outputs.

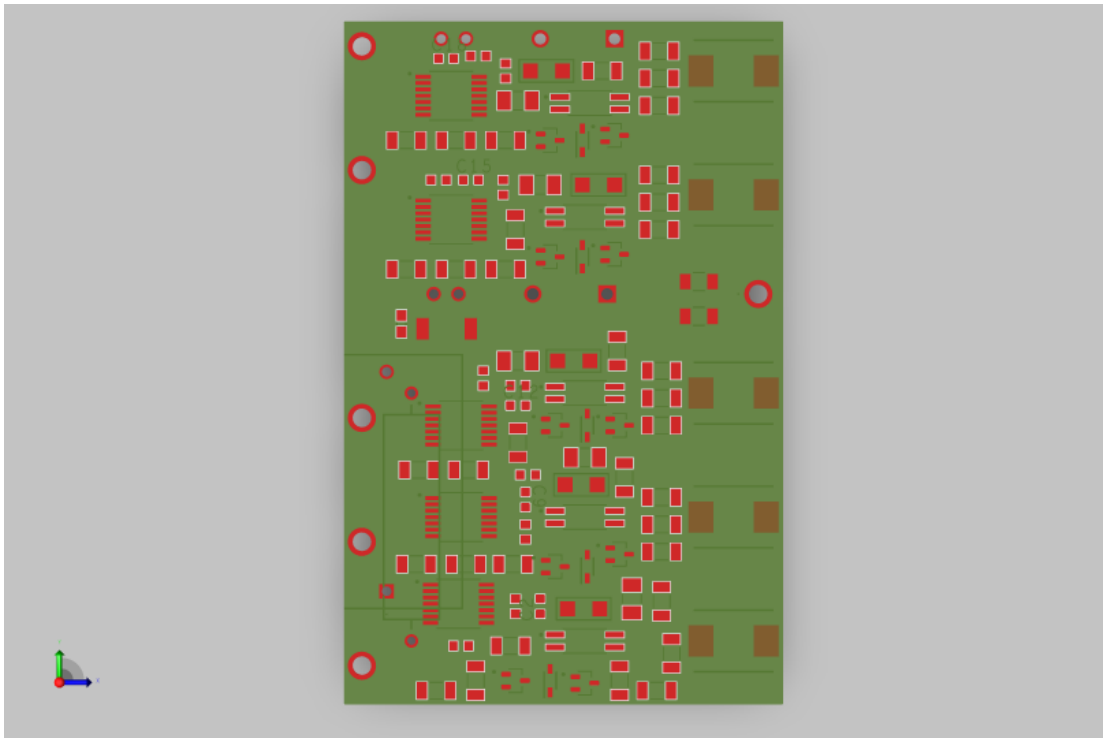

Fig. 4-3 PCB layout view for top side.

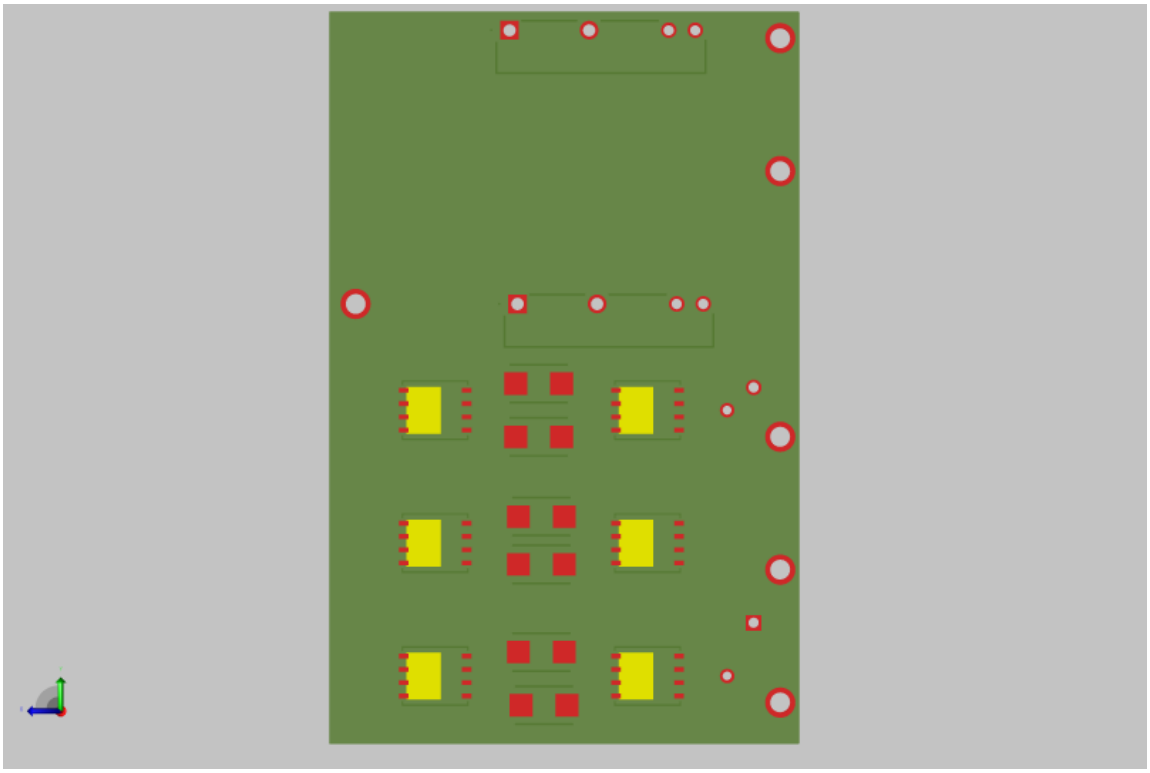

Fig. 4-4 PCB layout view for bottom side.

Additionally, a 3D view is presented for reference in Fig. 4-5 to Fig. 4-8. Pin-through-hole components, C1 Capacitor and L1 inductor on top side, as well as relays K1 & K2 on bottom side must be performed at 90° angle during board assembly to avoid housing collision, in this view these components were mapped as the original step model file.

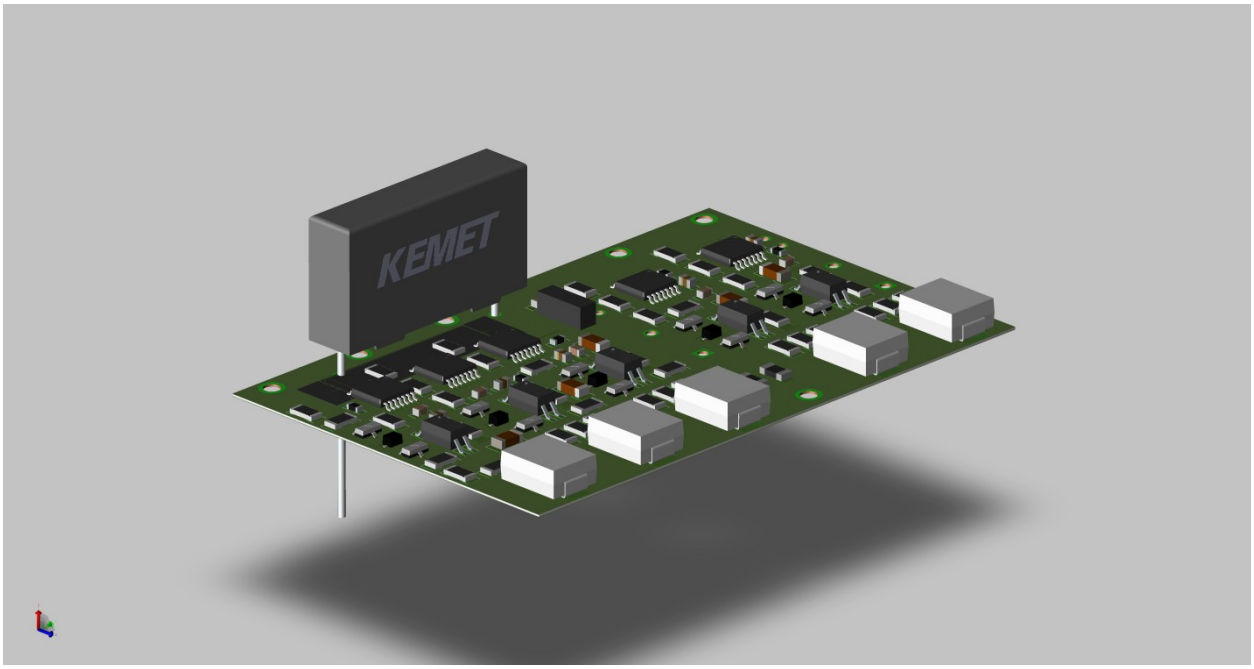

Fig. 4-5 Isometric top 3D view for PCB assembled board.

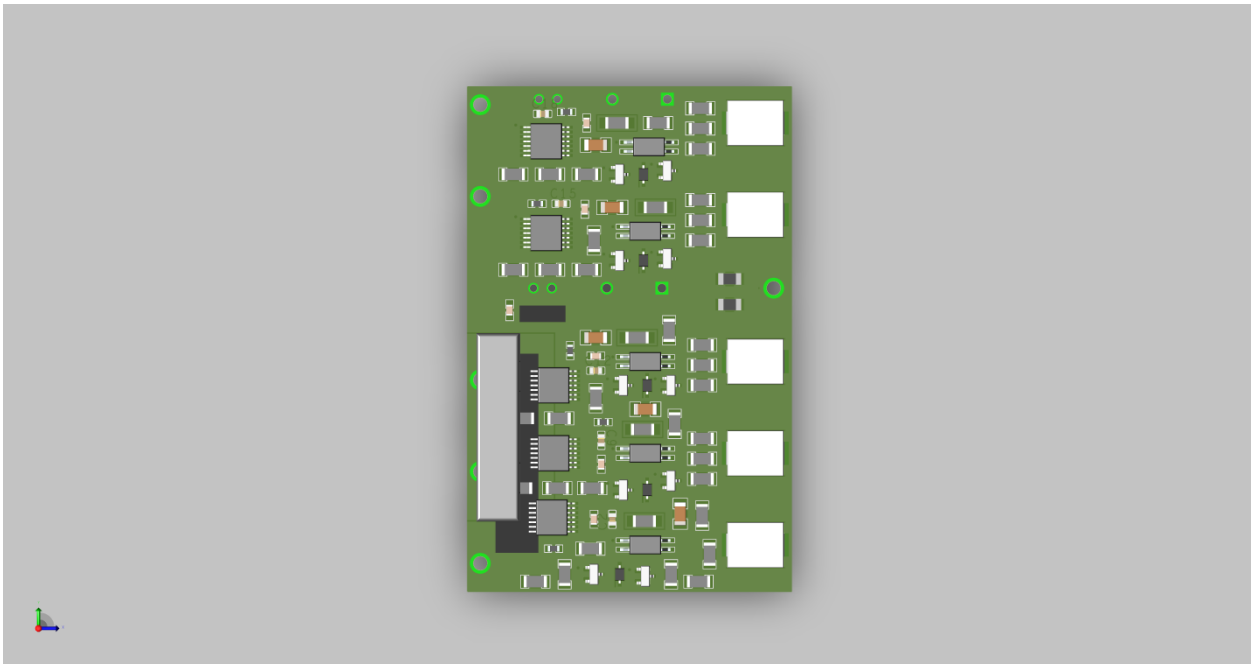

Fig. 4-6 Top 3D view for PCB assembled board.

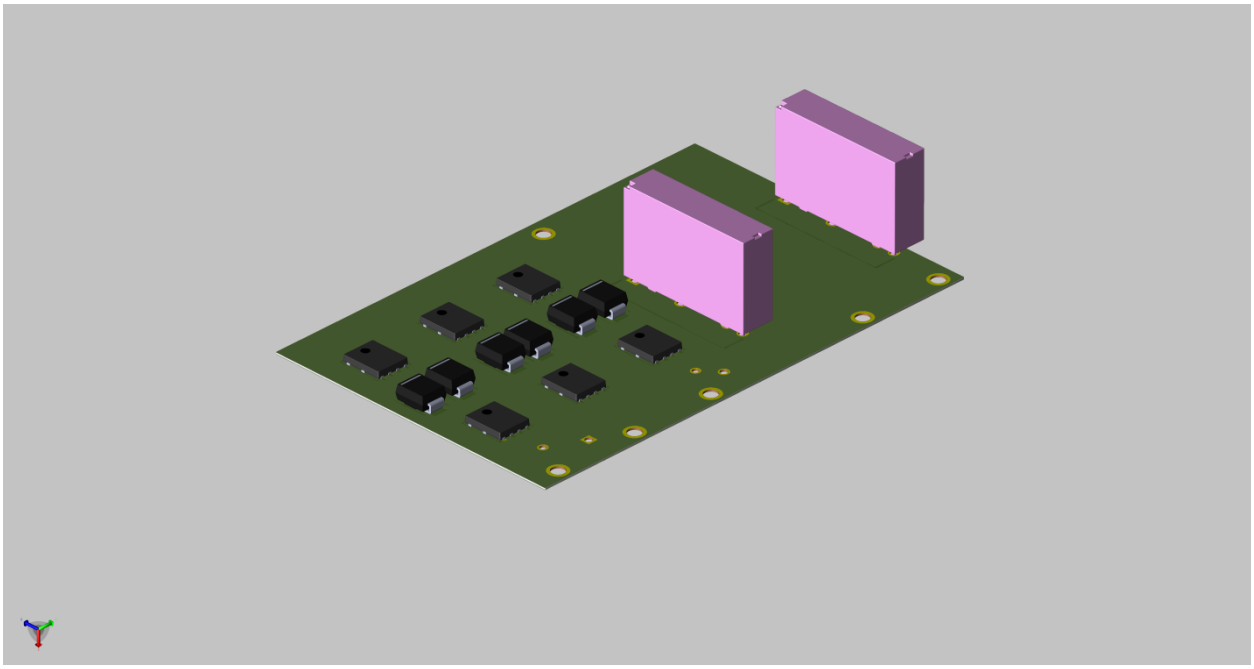

Fig. 4-7 Isometric bottom 3D view for PCB assembled board.

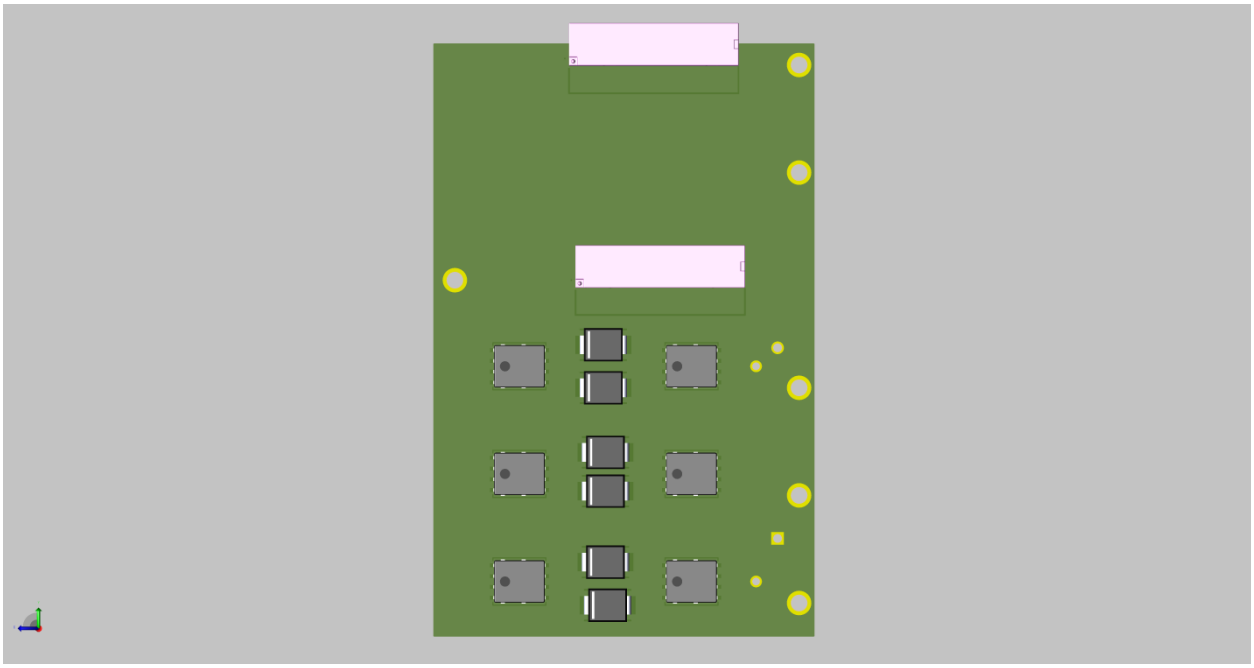

Fig. 4-8 Bottom 3D view for PCB assembled board.

Conclusion

In this work the process for a design upgrade of an intelligent controller module for building installations has been presented. The improvement was focused on increasing the amount of power outputs, increasing also the possibility of driving more loads on the same board.

The key element of this design upgrade was the downsizing of MOSFET devices. It was demonstrated that one smaller device can perform same function with 80% less space (DPAK to 5x6 MOSFET). Utilizing the suppliers' technology trends on component miniaturization, an optimal and very similar thermal behavior was achieved, however challenges on layout design are still present due to less footprint contact.

The Tj re-estimation by electrical measurements (junction to case estimation) and simulation also provided relevant information on MOSFET selection. The use of these tools allowed to save effort and money by predicting the thermal behavior. The comparison of worst-case analysis and simulation results allowed to reduce the margin error of selecting the replacement component.

Other challenges impacting on the layout space and cost of the implementation are related to relay protection. Even though this protection is essential for the product reliability, the market available components are not small enough nor cheap enough. A future effort concentrates on mapping suppliers' technology on component miniaturization and the establishment of different test cases scenarios with cost-effective components may reduce the total cost of the system implementation as a whole.

In a next stage, the complementary part of this work will be presented in a future work by my teammate Oswaldo Ramirez, focusing on the design upgrade of the logic board.

Appendix

A. Worst Case analysis UPU Power calculation

Version	Date	Author	Description
1.0	21-Mar-25	D. Gonzalez	First Release

Circuit:

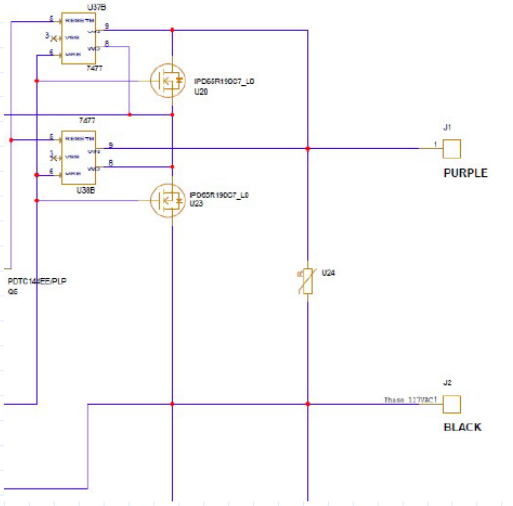

Specifications:

- Voltage: 220V AC
- Current: 3A RMS (300VA)
- Frequency: 60H
- Min-Max Resolution Duty Cycle range: 2-98%
- Temp: -10°C to 60°C

System Input Values:

Frequency System:

$Frequency := 60 \cdot Hz$

$Duty_{cycle} := 100$

$w := 2\ \pi \cdot Frequency$

Application Load:

$Load :=$ Resistive

$Rload := 36 \cdot \Omega$ $L_{ind} := 1 \cdot mH$

Ambient Temperature:

$T_A := 60$

Voltage System:

$V_{AC}(t) := 156\ \sin(w \cdot t) \cdot V$ 110V AC system

$RDSon := 0.3\ \Omega$

$V_{diode} := 0.7\ V$

General System Parameters:

$°C \equiv 1$

==========

Mosfet Characteristics:

Maximum RDSon at 25°C

$RDS_{on\_IPD65R190C7} := 0.168 \cdot \Omega$ Infineon - IPD65R190C7

$RDS_{on\_IPLK60R360PFD7} := 0.303 \cdot \Omega$ Infineon -IPLK60R360PFD7

$RDS_{on\_SiHJ240N60E} := 0.208 \cdot \Omega$ Vishay - SiHJ240N60E

$RDS_{on\_STL18N65M5} := 0.215 \cdot \Omega$ ST Micro - STL18N65M5

With the following equation the maximum and minimum RDSon of MOSFET is determined at -10°C and 60°C.

$$RDS_{on}\left(RDS_{on\_25°C}, \alpha, Tj\right) := RDS_{on\_25°C} \cdot \left(1 + \frac{\alpha}{100}\right)^{Tj - 25 \cdot °C}$$

$Th_C := 0.5$ RDSon thermal coeficient

$RDS_{on\_M1} := RDS_{on}\left(RDS_{on\_IPD65R190C7}, Th_C, T_A\right) = 0.2\ \Omega$ Infineon - IPD65R190C7

$RDS_{on\_M2} := RDS_{on}\left(RDS_{on\_IPLK60R360PFD7}, Th_C, T_A\right) = 0.361\ \Omega$ Infineon -IPLK60R360PFD7

$RDS_{on\_M3} := RDS_{on}\left(RDS_{on\_SiHJ240N60E}, Th_C, T_A\right) = 0.248\ \Omega$ Vishay - SiHJ240N60E

$RDS_{on\_M4} := RDS_{on}\left(RDS_{on\_STL18N65M5}, Th_C, T_A\right) = 0.256\ \Omega$ ST Micro - STL18N65M5

Thermal characteristics:

Case to Ambient thermal resistance:

$$R_{CA\_DPAK\_1L} := 62 \cdot \frac{K}{W}$$

$$R_{CA\_5x6\_1L} := 80 \cdot \frac{K}{W}$$

$$R_{CA\_DPAK\_M} := 25.3 \cdot \frac{K}{W}$$

$$R_{CA\_5x6\_M} := 32.6 \cdot \frac{K}{W}$$

Juntion to case thermal resistance:

$$Rth_{JC\_M1} := 1.73 \cdot \frac{K}{W}$$ Infineon - IPD65R190C7

$$Rth_{JC\_M2} := 1.70 \cdot \frac{K}{W}$$ Infineon -IPLK60R360PFD7

$$Rth_{JC\_M3} := 1.4 \cdot \frac{K}{W}$$ Vishay - SiHJ240N60E

$$Rth_{JC\_M4} := 2.2 \cdot \frac{K}{W}$$ ST Micro - STL18N65M5

Table 3 Thermal characteristics

Parameter	Symbol	Values			Unit	Note / Test Condition
		Min.	Typ.	Max.		
Thermal resistance, junction - case	R_{thJC}	-	-	1.73	°C/W	-
Thermal resistance, junction - ambient	R_{thJA}	-	-	62	°C/W	device on PCB, minimal footprint
Thermal resistance, junction - ambient for SMD version	R_{thJA}	-	35	45	°C/W	Device on 40mm*40mm*1.5mm epoxy PCB FR4 with 6cm² (one layer, 70µm thickness) copper area for drain connection and cooling. PCB is vertical without air stream cooling.
Soldering temperature, wave- & reflow soldering allowed	T_{sold}	-	-	260	°C	reflow MSL1

Table 3 Thermal characteristics

Parameter	Symbol	Values			Unit	Note / Test Condition
		Min.	Typ.	Max.		
Thermal resistance, junction - case	R_{thJC}	-	-	1.70	°C/W	-
Thermal resistance, junction - ambient	R_{thJA}	-	-	80	°C/W	device on PCB, minimal footprint
Thermal resistance, junction - ambient for SMD version	R_{thJA}	-	35	62	°C/W	Device on 40mm*40mm*1.5mm epoxy PCB FR4 with 6cm² (one layer, 70µm thickness) copper area for drain connection and cooling. PCB is vertical without air stream cooling.
Soldering temperature, wave & reflow soldering allowed	T_{sold}	-	-	260	°C	reflow MSL1

Charge characteristics:

$Q_{sw\_M1} := 7 \cdot nC$	$Q_{gs\_M1} := 6 \cdot nC$	$Q_{gtot\_M1} := 23 \cdot nC$	Infineon - IPD65R190C7
$Q_{sw\_M2} := 4.4 \cdot nC$	$Q_{gs\_M2} := 3 \cdot nC$	$Q_{gtot\_M2} := 12.7 \cdot nC$	Infineon -IPLK60R360PFD7
$Q_{sw\_M3} := 6 \cdot nC$	$Q_{gs\_M3} := 4 \cdot nC$	$Q_{gtot\_M3} := 15 \cdot nC$	Vishay - SiHJ240N60E
$Q_{sw\_M4} := 14 \cdot nC$	$Q_{gs\_M4} := 8 \cdot nC$	$Q_{gtot\_M4} := 31 \cdot nC$	ST Micro - STL18N65M5

Gate-Source Threshold Voltage (VTH)

VTH dependency with junction temperature:

$$VTH\_EVAL(VTH0, TC\_VTH, Tj) := VTH0 + TC\_VTH \cdot (Tj - 25)$$

$VTH_{M1} := VTH\_EVAL(3.5, -0.0018, T_A) = 3.437$	Infineon - IPD65R190C7	
$VTH_{M2} := VTH\_EVAL(4, -0.0018, T_A) = 3.937$	Infineon -IPLK60R360PFD7	VTH0 and TC obtained from datasheets
$VTH_{M3} := VTH\_EVAL(4, -0.0018, T_A) = 3.937$	Vishay - SiHJ240N60E	
$VTH_{M4} := VTH\_EVAL(4, -0.0018, T_A) = 3.937$	ST Micro - STL18N65M5	TC only available on STL18N65M5 (-0.0018) but used for all cases

Gate Voltage plateau: **(0.8V estimated from datasheets for ALL cases)**

$Vplateau_{M1} := VTH_{M1} \cdot V + 0.8 \cdot V = 4.237\ V$	Infineon - IPD65R190C7
$Vplateau_{M2} := VTH_{M1} \cdot V + 0.8 \cdot V = 4.237\ V$	Infineon -IPLK60R360PFD7
$Vplateau_{M3} := VTH_{M1} \cdot V + 0.8 \cdot V = 4.237\ V$	Vishay - SiHJ240N60E
$Vplateau_{M4} := VTH_{M1} \cdot V + 0.8 \cdot V = 4.237\ V$	ST Micro - STL18N65M5

NAND CD4093B Characteristics

$CD4093\_10V\_typ := 0.0026\ A$ $CD4093\_15V\_typ := 0.0068\ A$

$CD4093\_10V\_min := 0.0013\ A$ $CD4093\_15V\_min := 0.0034\ A$

GATE CURRENT CALCULATION:

$$CD4093\_delta\_typ := \frac{CD4093\_15V\_typ - CD4093\_10V\_typ}{5}$$

$$CD4093\_delta\_min := \frac{CD4093\_15V\_min - CD4093\_10V\_min}{5}$$

$$CD4093\_12V\_typ := CD4093\_10V\_typ + (2 \cdot CD4093\_delta\_typ)$$

$$CD4093\_12V\_min := CD4093\_10V\_min + (2 \cdot CD4093\_delta\_min)$$

$CD4093\_12V\_typ = 0.0043\ A$

$CD4093\_12V\_min = 0.0021\ A$

$CD4093\_12V\_max := CD4093\_12V\_typ + CD4093\_12V\_min$

$CD4093\_12V\_max = 0.0064\ A$ *CD4093_12V_max estimated from CD4093_12V_min and CD4093_12V_typ*

STATIC ELECTRICAL CHARACTERISTICS (CONT'D)

CHARACTERISTIC	CONDITIONS			LIMITS AT INDICATED TEMPERATURES (°C)							UNITS
	V_O (V)	V_{IN} (V)	V_{DD} (V)	-55	-40	+85	+125	+25 MIN.	+25 TYP.	+25 MAX.	
Output Low (Sink) Current, I_{OL} Min.	0.4	0.5	5	0.64	0.61	0.42	0.36	0.51	1	–	mA
	0.5	0.10	10	1.6	1.5	1.1	0.9	1.3	2.6	–	
	1.5	0.15	15	4.2	4	2.8	2.4	3.4	6.8	–	
Output High (Source) Current, I_{OH} Min.	4.6	0.5	5	-0.64	-0.61	-0.42	-0.36	-0.51	-1	–	
	2.5	0.5	5	-2	-1.8	-1.3	-1.15	-1.6	-3.2	–	
	9.5	0.10	10	-1.6	-1.5	-1.1	-0.9	-1.3	-2.6	–	
	13.5	0.15	15	-4.2	-4	-2.8	-2.4	-3.4	-6.8	–	
Output Voltage Low-Level, V_{OL} Max.	–	0.5	5	0.05				–	0	0.05	V
	–	0.10	10	0.05				–	0	0.05	
	–	0.15	15	0.05				–	0	0.05	
Output Voltage High-Level, V_{OH} Min.	–	0.5	5	4.95				4.95	5	–	
	–	0.10	10	9.95				9.95	10	–	
	–	0.15	15	14.95				14.95		–	
Input Current, I_{IN} Max.	–	0.18	18	±0.1	±0.1	±1	±1	–	$\pm 10^{-5}$	±0.1	μA

Load Current Behavior:

$$Period := \frac{1}{Frequency} = 16.667\ ms$$

$$t_{on\_pwm} := Duty_{cycle}\% \cdot Period = 16.667\ ms$$

$$t_{off\_pwm} := Period \cdot \left(\left|100 - Duty_{cycle}\right|\%\right) = 0\ ms$$

$$L_{ind} := \begin{cases} \text{if } Load = 2 \\ \quad 10 \cdot \mu H \\ \text{else} \\ \quad L_{ind} \end{cases}$$

$$times := \frac{Duty_{cycle}}{Frequency} = 1.667\ s$$

$$n\_cycles := \begin{cases} \text{if } Duty_{cycle} < 10 \\ \quad \text{floor}\left(\frac{\frac{L_{ind}}{Rload} \cdot 2}{times}\right) + 1 \\ \text{also if } Load = 2 \\ \quad \text{floor}\left(\frac{\frac{L_{ind}}{Rload} \cdot 2}{\frac{Period}{2}}\right) + 8 \\ \text{else} \\ \quad \text{floor}\left(\frac{\frac{L_{ind}}{Rload} \cdot 2}{\frac{Period}{2}}\right) + 8 \end{cases} = 8$$

Mosfet ON

$$i_{on\_load}(t, I_o) := \left(\frac{V_{AC}(t)}{Rload + RDSon}\right) + \left(\frac{-V_{AC}(t)}{Rload + RDSon}\right) \cdot e^{-\left(\frac{Rload}{L_{ind}}\right) \cdot t} + I_o \cdot e^{-\left(\frac{Rload}{L_{ind}}\right) \cdot t}$$

Mosfet OFF

$$i_{off\_load}(t, I_o) := \left(\frac{-V_{diode}}{Rload} + \left(I_o - \frac{-V_{diode}}{Rload} \right) \cdot e^{\frac{Rload \cdot -t}{L_{ind}}} \right)$$

$$i_{off\_B\_min}(t, I_o) := \begin{| if (i_{off\_load}(t, I_o)) \geq 0\ A \\ \quad i_{off\_load}(t, I_o) \\ if (i_{off\_load}(t, I_o)) < 0\ A \\ \quad 0\ A \end{|}$$

$$i_{load}(t) := \text{for } A \in 0 .. n\_cycles - 1$$
$$\begin{| if\ 0 < t \leq \left(\frac{Period}{2} \cdot Duty_{cycle} \right)\% \\ \quad i_{on\_load}(t, 0\ A) \\ if\ A \cdot Period + \left(\frac{Period}{2} \cdot Duty_{cycle} \right)\% < t \leq (A+1) \cdot \frac{Period}{2} \\ \quad i_{off\_B\_min}\left(t - \left(A \cdot Period + \left(\frac{Period}{2} \cdot Duty_{cycle} \right)\% \right), i_{load}\left(A \cdot Period + \left(\frac{Period}{2} \cdot Duty_{cycle} \right)\% \right) \right) \\ if\ (A+1) \cdot \frac{Period}{2} < t \leq (A+1) \cdot \frac{Period}{2} + \left(\frac{Period}{2} \cdot Duty_{cycle} \right)\% \\ \quad i_{on\_load}(t, 0\ A) \\ if\ (A+1) \cdot \frac{Period}{2} + \left(\frac{Period}{2} \cdot Duty_{cycle} \right)\% < t \leq (A+1) \cdot Period \\ \quad i_{off\_B\_min}\left(t - \left((A+1) \cdot \frac{Period}{2} + \left(\frac{Period}{2} \cdot Duty_{cycle} \right)\% \right), i_{load}\left((A+1) \cdot \frac{Period}{2} + \left(\frac{Period}{2} \cdot Duty_{cycle} \right)\% \right) \right) \end{|}$$

$$V_{rms} := \sqrt{\frac{1}{Period} \cdot \int_{\left(\frac{n\_cycles}{2} - 1\right) \cdot Period}^{\left(\frac{n\_cycles}{2}\right) \cdot Period} V_{AC}(t)^2 \, dt} = 110.309\ V$$

$$I_{rms} := \sqrt{\frac{1}{Period} \cdot \int_{\left(\frac{n\_cycles}{2} - 1\right) \cdot Period}^{\left(\frac{n\_cycles}{2}\right) \cdot Period} i_{load}(t)^2 \, dt} = 3.039\ A$$

$$V_{peak} := \left\| \begin{array}{l} \text{if } 0.1 \le Duty_{cycle} \le 99.9 \\ \quad \left\| V_{AC}\left(\left(\frac{Period}{2} \cdot Duty_{cycle}\right)\%\right) \right\| \\ \text{else} \\ \quad \left\| V_{AC}\left(\frac{Period}{4}\right) \right\| \end{array} \right\| = 156\ V$$

$$I_{peak} := \left\| \begin{array}{l} \text{if } 0.1 \le Duty_{cycle} \le 99.9 \\ \quad \left\| i_{load}\left(\left(\frac{Period}{2} \cdot Duty_{cycle}\right)\%\right) \right\| \\ \text{else} \\ \quad \left\| i_{load}\left(\frac{Period}{4}\right) \right\| \end{array} \right\| = 4.298\ A$$

$$t := 0\ s, \frac{(Period \cdot n\_cycles) \cdot 2\ \pi}{10000} .. Period \cdot n\_cycles \cdot 2\ \pi$$

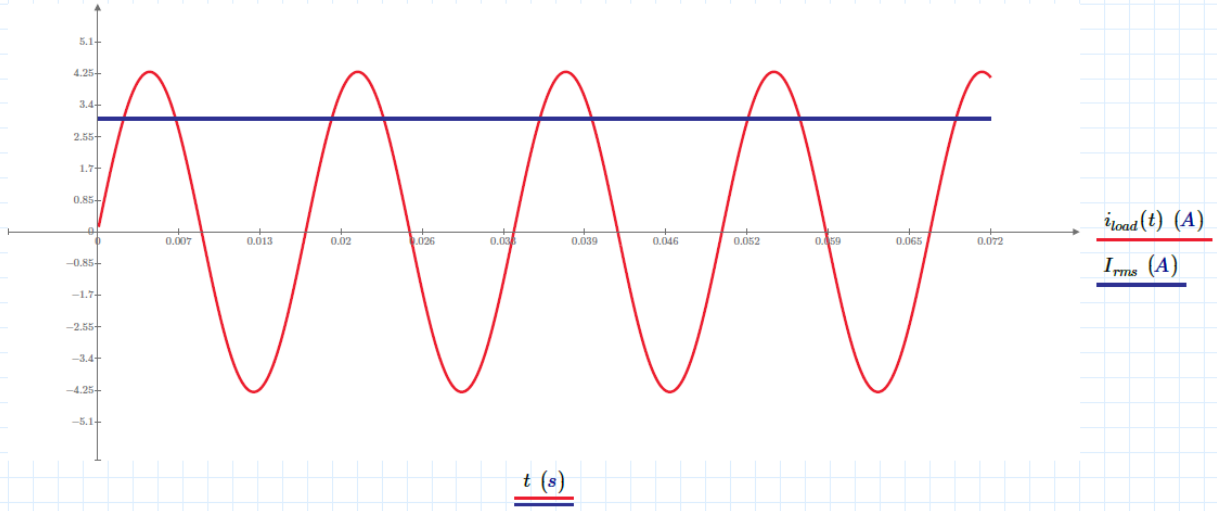

Power calculation when mosfet is in on state:

$$MOS_{Power\_on\_M1} := RDS_{on\_M1} \cdot \frac{1}{Period} \cdot \left(\int_{Period \cdot \frac{n\_cycles}{2} - Period}^{t_{on\_pwm} + \left(Period \cdot \frac{n\_cycles}{2} - Period \right)} i_{load}(t)^2 \, dt \right) = 1.847\ W$$

Infineon - IPD65R190C7

$$MOS_{Power\_on\_M2} := RDS_{on\_M2} \cdot \frac{1}{Period} \cdot \left(\int_{Period \cdot \frac{n\_cycles}{2} - Period}^{t_{on\_pwm} + \left(Period \cdot \frac{n\_cycles}{2} - Period \right)} i_{load}(t)^2 \, dt \right) = 3.332\ W$$

Infineon -IPLK60R360PFD7

$$MOS_{Power\_on\_M3} := RDS_{on\_M3} \cdot \frac{1}{Period} \cdot \left(\int_{Period \cdot \frac{n\_cycles}{2} - Period}^{t_{on\_pwm} + \left(Period \cdot \frac{n\_cycles}{2} - Period \right)} i_{load}(t)^2 \, dt \right) = 2.287\ W$$

Vishay - SiHJ240N60E

$$MOS_{Power\_on\_M4} := RDS_{on\_M4} \cdot \frac{1}{Period} \cdot \left(\int_{Period \cdot \frac{n\_cycles}{2} - Period}^{t_{on\_pwm} + \left(Period \cdot \frac{n\_cycles}{2} - Period \right)} i_{load}(t)^2 \, dt \right) = 2.364\ W$$

ST Micro - STL18N65M5

Gate current calculation:

Gate resistance: $Rgate\_typ := 47 \cdot \Omega$ $Rgate\_max := Rgate\_typ \cdot 1.03$ $Rgate\_min := Rgate\_typ \cdot 0.97$

Gate Charge Current: $GCC\_ON\_typ := CD4093\_12V\_typ$ $GCC\_OFF\_typ := CD4093\_12V\_typ$

$GCC\_ON\_min := CD4093\_12V\_min$ $GCC\_OFF\_min := CD4093\_12V\_min$

$GCC\_ON\_max := CD4093\_12V\_max$ $GCC\_OFF\_max := CD4093\_12V\_max$

47ohm resistance is neglected in this calculation

Switch Time Calculation:

$$Tsw(Qsw, GCC) := \frac{Qsw}{GCC}$$

Infineon - IPD65R190C7

ON PHASE

$T_{dON\_min\_M1} := Tsw(Q_{gs\_M1}, GCC\_ON\_max) = 0.935\ \mu s$

$T_{dON\_typ\_M1} := Tsw(Q_{gs\_M1}, GCC\_ON\_typ) = 1.402\ \mu s$

$T_{dON\_max\_M1} := Tsw(Q_{gs\_M1}, GCC\_ON\_min) = 2.804\ \mu s$

$T_{swON\_min\_M1} := Tsw(Q_{sw\_M1}, GCC\_ON\_max) = 1.09\ \mu s$

$T_{swON\_typ\_M1} := Tsw(Q_{sw\_M1}, GCC\_ON\_typ) = 1.636\ \mu s$

$T_{swON\_max\_M1} := Tsw(Q_{sw\_M1}, GCC\_ON\_min) = 3.271\ \mu s$

$$SR\_ON\_min\_M1 := \frac{V_{peak}}{T_{swON\_max\_M1}} = 47.691\ \frac{V}{\mu s}$$

$$SR\_ON\_typ\_M1 := \frac{V_{peak}}{T_{swON\_typ\_M1}} = 95.383\ \frac{V}{\mu s}$$

$$SR\_ON\_max\_M1 := \frac{V_{peak}}{T_{swON\_min\_M1}} = 143.074\ \frac{V}{\mu s}$$

OFF PHASE

$T_{dOFF\_min\_M1} := Tsw(Q_{gtot\_M1} - Q_{gs\_M1} - Q_{sw\_M1}, GCC\_ON\_max) = 1.558\ \mu s$

$T_{dOFF\_typ\_M1} := Tsw(Q_{gtot\_M1} - Q_{gs\_M1} - Q_{sw\_M1}, GCC\_OFF\_typ) = 2.336\ \mu s$

$T_{dOFF\_max\_M1} := Tsw(Q_{gtot\_M1} - Q_{gs\_M1} - Q_{sw\_M1}, GCC\_OFF\_min) = 4.673\ \mu s$

$T_{swOFF\_min\_M1} := Tsw(Q_{sw\_M1}, GCC\_ON\_max) = 1.09\ \mu s$

$T_{swOFF\_typ\_M1} := Tsw(Q_{sw\_M1}, GCC\_OFF\_typ) = 1.636\ \mu s$

$T_{swOFF\_max\_M1} := Tsw(Q_{sw\_M1}, GCC\_OFF\_min) = 3.271\ \mu s$

$$SR\_OFF\_min\_M1 := \frac{V_{peak}}{T_{swOFF\_max\_M1}} = 47.691\ \frac{V}{\mu s}$$

$$SR\_OFF\_typ\_M1 := \frac{V_{peak}}{T_{swOFF\_typ\_M1}} = 95.383\ \frac{V}{\mu s}$$

$$SR\_OFF\_max\_M1 := \frac{V_{peak}}{T_{swOFF\_min\_M1}} = 143.074\ \frac{V}{\mu s}$$

Power losses during switching:

$$Power_{sw\_max\_M1} := \left| \begin{array}{l} \text{if } 0.1 \le Duty_{cycle} \le 99.9 \\ \quad \left| \frac{1}{2} \cdot \left(T_{swON\_max\_M1} + T_{swOFF\_max\_M1}\right) \cdot \left(V_{peak} + V_{diode}\right) \cdot I_{rms} \cdot Frequency \right| \\ \text{else} \\ \quad |0 \cdot W| \end{array} \right| = 0\ W$$

$$Power_{sw\_min\_M1} := \left| \begin{array}{l} \text{if } 0.1 \le Duty_{cycle} \le 99.9 \\ \quad \left| \frac{1}{2} \cdot \left(T_{swON\_min\_M1} + T_{swOFF\_min\_M1}\right) \cdot \left(V_{peak} + V_{diode}\right) \cdot I_{rms} \cdot Frequency \right| \\ \text{else} \\ \quad |0 \cdot W| \end{array} \right| = 0\ W$$

$$Power_{sw\_typ\_M1} := \left| \begin{array}{l} \text{if } 0.1 \le Duty_{cycle} \le 99.9 \\ \quad \left| \frac{1}{2} \cdot \left(T_{swON\_typ\_M1} + T_{swOFF\_typ\_M1}\right) \cdot \left(V_{peak} + V_{diode}\right) \cdot I_{rms} \cdot Frequency \right| \\ \text{else} \\ \quad |0 \cdot W| \end{array} \right| = 0\ W$$

Power losses in the MOSFET can be expressed as the sum of conduction and switching losses:
Ptot = Pconduction + Pswitch

$$P_{total}\left(P_{cond}, P_{swtich}\right) := P_{cond} + P_{swtich}$$

$$P_{total\_max\_M1} := P_{total}\left(MOS_{Power\_on\_M1}, Power_{sw\_max\_M1}\right) = 1.847\ W$$

$$P_{total\_min\_M1} := P_{total}\left(MOS_{Power\_on\_M1}, Power_{sw\_min\_M1}\right) = 1.847\ W$$

$$P_{total\_typ\_M1} := P_{total}\left(MOS_{Power\_on\_M1}, Power_{sw\_typ\_M1}\right) = 1.847\ W$$

Infineon -IPLK60R360PFD7

ON PHASE

$T_{dON\_min\_M2} := Tsw\left(Q_{gs\_M2}, GCC\_ON\_max\right) = 0.467\ \mu s$

$T_{dON\_typ\_M2} := Tsw\left(Q_{gs\_M2}, GCC\_ON\_typ\right) = 0.701\ \mu s$

$T_{dON\_max\_M2} := Tsw\left(Q_{gs\_M2}, GCC\_ON\_min\right) = 1.402\ \mu s$

$T_{swON\_min\_M2} := Tsw\left(Q_{sw\_M2}, GCC\_ON\_max\right) = 0.685\ \mu s$

$T_{swON\_typ\_M2} := Tsw\left(Q_{sw\_M2}, GCC\_ON\_typ\right) = 1.028\ \mu s$

$T_{swON\_max\_M2} := Tsw\left(Q_{sw\_M2}, GCC\_ON\_min\right) = 2.056\ \mu s$

$SR\_ON\_min\_M2 := \frac{V_{peak}}{T_{swON\_max\_M2}} = 75.873\ \frac{V}{\mu s}$

$SR\_ON\_typ\_M2 := \frac{V_{peak}}{T_{swON\_typ\_M2}} = 151.745\ \frac{V}{\mu s}$

$SR\_ON\_max\_M2 := \frac{V_{peak}}{T_{swON\_min\_M2}} = 227.618\ \frac{V}{\mu s}$

OFF PHASE

$T_{dOFF\_min\_M2} := Tsw\left(Q_{gtot\_M2} - Q_{gs\_M2} - Q_{sw\_M2}, GCC\_ON\_max\right) = 0.826\ \mu s$

$T_{dOFF\_typ\_M2} := Tsw\left(Q_{gtot\_M2} - Q_{gs\_M2} - Q_{sw\_M2}, GCC\_OFF\_typ\right) = 1.238\ \mu s$

$T_{dOFF\_max\_M2} := Tsw\left(Q_{gtot\_M2} - Q_{gs\_M2} - Q_{sw\_M2}, GCC\_OFF\_min\right) = 2.477\ \mu s$

$T_{swOFF\_min\_M2} := Tsw\left(Q_{sw\_M2}, GCC\_ON\_max\right) = 0.685\ \mu s$

$T_{swOFF\_typ\_M2} := Tsw\left(Q_{sw\_M2}, GCC\_OFF\_typ\right) = 1.028\ \mu s$

$T_{swOFF\_max\_M2} := Tsw\left(Q_{sw\_M2}, GCC\_OFF\_min\right) = 2.056\ \mu s$

$SR\_OFF\_min\_M2 := \frac{V_{peak}}{T_{swOFF\_max\_M2}} = 75.873\ \frac{V}{\mu s}$

$SR\_OFF\_typ\_M2 := \frac{V_{peak}}{T_{swOFF\_typ\_M2}} = 151.745\ \frac{V}{\mu s}$

$SR\_OFF\_max\_M2 := \frac{V_{peak}}{T_{swOFF\_min\_M2}} = 227.618\ \frac{V}{\mu s}$

Power losses during switching:

$$Power_{sw\_max\_M2} := \left| \begin{array}{l} \text{if } 0.1 \le Duty_{cycle} \le 99.9 \\ \quad \left| \frac{1}{2} \cdot \left(T_{swON\_max\_M2} + T_{swOFF\_max\_M2}\right) \cdot \left(V_{peak} + V_{diode}\right) \cdot I_{rms} \cdot Frequency \right| \\ \text{else} \\ \quad \left| 0 \cdot W \right| \end{array} \right| = 0\ W$$

$$Power_{sw\_min\_M2} := \left| \begin{array}{l} \text{if } 0.1 \le Duty_{cycle} \le 99.9 \\ \quad \left| \frac{1}{2} \cdot \left(T_{swON\_min\_M2} + T_{swOFF\_min\_M2}\right) \cdot \left(V_{peak} + V_{diode}\right) \cdot I_{rms} \cdot Frequency \right| \\ \text{else} \\ \quad \left| 0 \cdot W \right| \end{array} \right| = 0\ W$$

$$Power_{sw\_typ\_M2} := \left| \begin{array}{l} \text{if } 0.1 \le Duty_{cycle} \le 99.9 \\ \quad \left| \frac{1}{2} \cdot \left(T_{swON\_typ\_M2} + T_{swOFF\_typ\_M2}\right) \cdot \left(V_{peak} + V_{diode}\right) \cdot I_{rms} \cdot Frequency \right| \\ \text{else} \\ \quad \left| 0 \cdot W \right| \end{array} \right| = 0\ W$$

Power losses in the MOSFET can be expressed as the sum of conduction and switching losses:
Ptot = Pconduction + Pswitch

$$P_{total\_max\_M2} := P_{total}\left(MOS_{Power\_on\_M2}, Power_{sw\_max\_M2}\right) = 3.332\ W$$

$$P_{total\_min\_M2} := P_{total}\left(MOS_{Power\_on\_M2}, Power_{sw\_min\_M2}\right) = 3.332\ W$$

$$P_{total\_typ\_M2} := P_{total}\left(MOS_{Power\_on\_M2}, Power_{sw\_typ\_M2}\right) = 3.332\ W$$

Vishay - SiHJ240N60E

ON PHASE

$T_{dON\_min\_M3} := Tsw\left(Q_{gs\_M3}, GCC\_ON\_max\right) = 0.623\ \mu s$

$T_{dON\_typ\_M3} := Tsw\left(Q_{gs\_M3}, GCC\_ON\_typ\right) = 0.935\ \mu s$

$T_{dON\_max\_M3} := Tsw\left(Q_{gs\_M3}, GCC\_ON\_min\right) = 1.869\ \mu s$

$T_{swON\_min\_M3} := Tsw\left(Q_{sw\_M3}, GCC\_ON\_max\right) = 0.935\ \mu s$

$T_{swON\_typ\_M3} := Tsw\left(Q_{sw\_M3}, GCC\_ON\_typ\right) = 1.402\ \mu s$

$T_{swON\_max\_M3} := Tsw\left(Q_{sw\_M3}, GCC\_ON\_min\right) = 2.804\ \mu s$

$SR\_ON\_min\_M3 := \frac{V_{peak}}{T_{swON\_max\_M3}} = 55.64\ \frac{V}{\mu s}$

$SR\_ON\_typ\_M3 := \frac{V_{peak}}{T_{swON\_typ\_M3}} = 111.28\ \frac{V}{\mu s}$

$SR\_ON\_max\_M3 := \frac{V_{peak}}{T_{swON\_min\_M3}} = 166.92\ \frac{V}{\mu s}$

OFF PHASE

$T_{dOFF\_min\_M3} := Tsw\left(Q_{gtot\_M3} - Q_{gs\_M3} - Q_{sw\_M3}, GCC\_ON\_max\right) = 0.779\ \mu s$

$T_{dOFF\_typ\_M3} := Tsw\left(Q_{gtot\_M3} - Q_{gs\_M3} - Q_{sw\_M3}, GCC\_OFF\_typ\right) = 1.168\ \mu s$

$T_{dOFF\_max\_M3} := Tsw\left(Q_{gtot\_M3} - Q_{gs\_M3} - Q_{sw\_M3}, GCC\_OFF\_min\right) = 2.336\ \mu s$

$T_{swOFF\_min\_M3} := Tsw\left(Q_{sw\_M3}, GCC\_ON\_max\right) = 0.935\ \mu s$

$T_{swOFF\_typ\_M3} := Tsw\left(Q_{sw\_M3}, GCC\_OFF\_typ\right) = 1.402\ \mu s$

$T_{swOFF\_max\_M3} := Tsw\left(Q_{sw\_M3}, GCC\_OFF\_min\right) = 2.804\ \mu s$

$SR\_OFF\_min\_M3 := \frac{V_{peak}}{T_{swOFF\_max\_M3}} = 55.64\ \frac{V}{\mu s}$

$SR\_OFF\_typ\_M3 := \frac{V_{peak}}{T_{swOFF\_typ\_M3}} = 111.28\ \frac{V}{\mu s}$

$SR\_OFF\_max\_M3 := \frac{V_{peak}}{T_{swOFF\_min\_M3}} = 166.92\ \frac{V}{\mu s}$

Power losses during switching:

$$Power_{sw\_max\_M3} := \left| \begin{array}{l} \text{if } 0.1 \le Duty_{cycle} \le 99.9 \\ \quad \left| \frac{1}{2} \cdot \left(T_{swON\_max\_M3} + T_{swOFF\_max\_M3}\right) \cdot \left(V_{peak} + V_{diode}\right) \cdot I_{rms} \cdot Frequency \right| \\ \text{else} \\ \quad |0 \cdot W| \end{array} \right| = 0\ W$$

$$Power_{sw\_min\_M3} := \left| \begin{array}{l} \text{if } 0.1 \le Duty_{cycle} \le 99.9 \\ \quad \left| \frac{1}{2} \cdot \left(T_{swON\_min\_M3} + T_{swOFF\_min\_M3}\right) \cdot \left(V_{peak} + V_{diode}\right) \cdot I_{rms} \cdot Frequency \right| \\ \text{else} \\ \quad |0 \cdot W| \end{array} \right| = 0\ W$$

$$Power_{sw\_typ\_M3} := \left| \begin{array}{l} \text{if } 0.1 \le Duty_{cycle} \le 99.9 \\ \quad \left| \frac{1}{2} \cdot \left(T_{swON\_typ\_M3} + T_{swOFF\_typ\_M3}\right) \cdot \left(V_{peak} + V_{diode}\right) \cdot I_{rms} \cdot Frequency \right| \\ \text{else} \\ \quad |0 \cdot W| \end{array} \right| = 0\ W$$

Power losses in the MOSFET can be expressed as the sum of conduction and switching losses:
Ptot = Pconduction + Pswitch

$$P_{total\_max\_M3} := P_{total}\left(MOS_{Power\_on\_M3}, Power_{sw\_max\_M3}\right) = 2.287\ W$$

$$P_{total\_min\_M3} := P_{total}\left(MOS_{Power\_on\_M3}, Power_{sw\_min\_M3}\right) = 2.287\ W$$

$$P_{total\_typ\_M3} := P_{total}\left(MOS_{Power\_on\_M3}, Power_{sw\_typ\_M3}\right) = 2.287\ W$$

ST Micro - STL18N65M5

ON PHASE

$T_{dON\_min\_M4} := Tsw\left(Q_{gs\_M4}, GCC\_ON\_max\right) = 1.246\ \mu s$

$T_{dON\_typ\_M4} := Tsw\left(Q_{gs\_M4}, GCC\_ON\_typ\right) = 1.869\ \mu s$

$T_{dON\_max\_M4} := Tsw\left(Q_{gs\_M4}, GCC\_ON\_min\right) = 3.738\ \mu s$

$T_{swON\_min\_M4} := Tsw\left(Q_{sw\_M4}, GCC\_ON\_max\right) = 2.181\ \mu s$

$T_{swON\_typ\_M4} := Tsw\left(Q_{sw\_M4}, GCC\_ON\_typ\right) = 3.271\ \mu s$

$T_{swON\_max\_M4} := Tsw\left(Q_{sw\_M4}, GCC\_ON\_min\right) = 6.542\ \mu s$

$SR\_ON\_min\_M4 := \frac{V_{peak}}{T_{swON\_max\_M4}} = 23.846\ \frac{V}{\mu s}$

$SR\_ON\_typ\_M4 := \frac{V_{peak}}{T_{swON\_typ\_M4}} = 47.691\ \frac{V}{\mu s}$

$SR\_ON\_max\_M4 := \frac{V_{peak}}{T_{swON\_min\_M4}} = 71.537\ \frac{V}{\mu s}$

OFF PHASE

$T_{dOFF\_min\_M4} := Tsw\left(Q_{gtot\_M4} - Q_{gs\_M4} - Q_{sw\_M4}, GCC\_ON\_max\right) = 1.402\ \mu s$

$T_{dOFF\_typ\_M4} := Tsw\left(Q_{gtot\_M4} - Q_{gs\_M4} - Q_{sw\_M4}, GCC\_OFF\_typ\right) = 2.103\ \mu s$

$T_{dOFF\_max\_M4} := Tsw\left(Q_{gtot\_M4} - Q_{gs\_M4} - Q_{sw\_M4}, GCC\_OFF\_min\right) = 4.206\ \mu s$

$T_{swOFF\_min\_M4} := Tsw\left(Q_{sw\_M4}, GCC\_ON\_max\right) = 2.181\ \mu s$

$T_{swOFF\_typ\_M4} := Tsw\left(Q_{sw\_M4}, GCC\_OFF\_typ\right) = 3.271\ \mu s$

$T_{swOFF\_max\_M4} := Tsw\left(Q_{sw\_M4}, GCC\_OFF\_min\right) = 6.542\ \mu s$

$SR\_OFF\_min\_M4 := \frac{V_{peak}}{T_{swOFF\_max\_M4}} = 23.846\ \frac{V}{\mu s}$

$SR\_OFF\_typ\_M4 := \frac{V_{peak}}{T_{swOFF\_typ\_M4}} = 47.691\ \frac{V}{\mu s}$

$SR\_OFF\_max\_M4 := \frac{V_{peak}}{T_{swOFF\_min\_M4}} = 71.537\ \frac{V}{\mu s}$

Power losses during switching:

$$Power_{sw\_max\_M4} := \left\| \begin{array}{l} \text{if } 0.1 \le Duty_{cycle} \le 99.9 \\ \quad \left\| \frac{1}{2} \cdot \left(T_{swON\_max\_M4} + T_{swOFF\_max\_M4}\right) \cdot \left(V_{peak} + V_{diode}\right) \cdot I_{rms} \cdot Frequency \right\| \\ \text{else} \\ \quad \| 0 \cdot W \end{array} \right\| = 0\ W$$

$$Power_{sw\_min\_M4} := \left\| \begin{array}{l} \text{if } 0.1 \le Duty_{cycle} \le 99.9 \\ \quad \left\| \frac{1}{2} \cdot \left(T_{swON\_min\_M4} + T_{swOFF\_min\_M4}\right) \cdot \left(V_{peak} + V_{diode}\right) \cdot I_{rms} \cdot Frequency \right\| \\ \text{else} \\ \quad \| 0 \cdot W \end{array} \right\| = 0\ W$$

$$Power_{sw\_typ\_M4} := \left\| \begin{array}{l} \text{if } 0.1 \le Duty_{cycle} \le 99.9 \\ \quad \left\| \frac{1}{2} \cdot \left(T_{swON\_typ\_M4} + T_{swOFF\_typ\_M4}\right) \cdot \left(V_{peak} + V_{diode}\right) \cdot I_{rms} \cdot Frequency \right\| \\ \text{else} \\ \quad \| 0 \cdot W \end{array} \right\| = 0\ W$$

Power losses in the MOSFET can be expressed as the sum of conduction and switching losses:
Ptot = Pconduction + Pswitch

$$P_{total\_max\_M4} := P_{total}\left(MOS_{Power\_on\_M4}, Power_{sw\_max\_M4}\right) = 2.364\ W$$

$$P_{total\_min\_M4} := P_{total}\left(MOS_{Power\_on\_M4}, Power_{sw\_min\_M4}\right) = 2.364\ W$$

$$P_{total\_typ\_M4} := P_{total}\left(MOS_{Power\_on\_M4}, Power_{sw\_typ\_M4}\right) = 2.364\ W$$

Thermal Behavior:

From the thermal model of the single MOSFET shown below, the following equations are used to obtain the junction temperature of MOSFET and PCB temperatures.

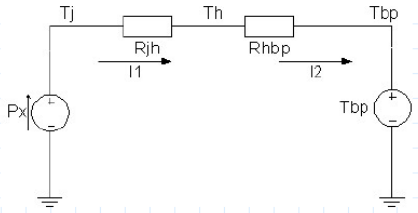

Junction temperature of MOSFET

$$Tjs(Px, Rjh, Rhbp, Tbp) := Px \cdot Rjh + Px \cdot Rhbp + Tbp$$

PCB temperature underneat MOSFET Baseplate

$$Th(Px, Rhbp, Tbp) := Px \cdot Rhbp + Tbp$$

$Temp_{solder\_max\_M1} := Th(P_{total\_max\_M1}, Rth_{JC\_M1}, T_A \cdot K) = 63.196\ K$

Infineon - IPD65R190C7

$Temp_{junction\_max\_M1} := Tjs(P_{total\_max\_M1}, Rth_{JC\_M1}, R_{CA\_DPAK\_M}, T_A \cdot K) = 109.931\ K$

$Temp_{solder\_max\_M2} := Th(P_{total\_max\_M2}, Rth_{JC\_M2}, T_A \cdot K) = 65.664\ K$

Infineon - IPLK60R360PFD7

$Temp_{junction\_max\_M2} := Tjs(P_{total\_max\_M2}, Rth_{JC\_M2}, R_{CA\_5x6\_M}, T_A \cdot K) = 174.276\ K$

$Temp_{solder\_max\_M3} := Th(P_{total\_max\_M3}, Rth_{JC\_M3}, T_A \cdot K) = 63.202\ K$

Vishay - SiHJ240N60E

$Temp_{junction\_max\_M3} := Tjs(P_{total\_max\_M3}, Rth_{JC\_M3}, R_{CA\_5x6\_M}, T_A \cdot K) = 137.761\ K$

$Temp_{solder\_max\_M4} := Th(P_{total\_max\_M4}, Rth_{JC\_M4}, T_A \cdot K) = 65.201\ K$

ST Micro - STL18N65M5

$Temp_{junction\_max\_M4} := Tjs(P_{total\_max\_M4}, Rth_{JC\_M4}, R_{CA\_5x6\_M}, T_A \cdot K) = 142.269\ K$

Summary:

LOAD CONDITION					
VRMS (V)	110.31	Frequency (hz)	60	Duty (%)	100
IRMS (A)	3.04	IPEAK (A)	4.30	VPEAK (V)	156.00

$T_A = 60$

MOSFET RESULTS												
Supplier / Package	Infineon - IPD65R190C7 DPAK			Infineon - IPLK60R360PFD7 ThinPAK 5x6			Vishay - SiHJ240N60E PowerPAK SO-8L			ST Micro - STL18N65M5 PowerFLAT 5x6 HV		
Parameter	min	typ	max	min	typ	max	min	typ	max	min	typ	max
Slew-Rate ON (V/us)	47.691	95.383	143.074	75.873	151.745	227.618	55.640	111.280	166.920	23.846	47.691	71.537
Slew-Rate OFF (V/us)	47.691	95.383	143.074	75.873	151.745	227.618	55.640	111.280	166.920	23.846	47.691	71.537
Conduction Losses (W)	1.847	1.847	1.847	3.332	3.332	3.332	2.287	2.287	2.287	2.364	2.364	2.364
Switching Losses (W)	0.000	0.000	0.000	0.000	0.000	0.000	0.000	0.000	0.000	0.000	0.000	0.000
Total Losess (W)	1.847	1.847	1.847	3.332	3.332	3.332	2.287	2.287	2.287	2.364	2.364	2.364
Max. Tamb (°C)	60.000			60.000			60.000			60.000		
Max. Tsolder (°C)	63.196			65.664			63.202			65.201		
Max. Tjunction (°C)	109.931			174.276			137.761			142.269		

Worst case scenario is 100% DC ==> 3A RMS, Ta=60C

Result:
Due max Tjunction estimated (178C) seems the value of RthCA should be less than 62 K/W for current design (DPAK mosfet), otherwise mosfet would not withstant the max Tjunction allowed (150C).

Action:
New RthCA estimation should be done for DPAK and 5x6 packages to get a reliable estimation. ===> Completed: 04-Oct-2025

New value for RthCA DPAK = 25.3 K/W
New value for RthCA 5x6 = 32.6 K/W

B. COSTED BOM (OLD VS. NEW)

- Old BOM (Quoted prices per 100 pieces from Mouser, Digikey, PCB Way and TME Electronic components on Nov 24th, 2025)

Qty	Value	Part Function	Package	Supplier name	Supplier part number	Price (per 100)	Price	Currency
1	CU3225K275G2	Varistor	3225	TDK	B72650M0271K072	$55.30	$0.55	USD
1	IPD65R190C7	Mosfet	DPAK	Infineon	IPD65R190C7ATMA1	$173.00	$1.73	USD
1	IPD65R190C7	Mosfet	DPAK	Infineon	IPD65R190C7ATMA1	$173.00	$1.73	USD
1	"unknow component"	"unknow component"	SOT323-5	"unknow component"	"unknow component"	$28.90	$0.29	USD
1	"unknow component"	"unknow component"	SOT323-5	"unknow component"	"unknow component"	$28.90	$0.29	USD
1	47	Resistor	0603	Vishay	CRCW060347R0JNEAC	$1.20	$0.01	USD
1	CD4093B	NAND	TSSOP14	Texas Instrument	CD4093BPWR	$59.80	$0.60	USD
1	HMHA2801	Optocoupler	MPF4	Onsemi	HMHA2801	$36.80	$0.37	USD
1	100k	Resistor	0603	Vishay	CRCW0603100KJNEAC	$1.00	$0.01	USD
1	1n	Capacitor	0603	Samsung Electro-Mechanics	CL10B102KC8NNWC	$2.60	$0.03	USD
1	PDTC144EE	Transistor	SOT416	Nexperia	PDTC144ET	$8.20	$0.08	USD
1	220k	Resistor	0603	Vishay	CRCW0603220KFKEAC	$1.30	$0.01	USD
1	56n	Capacitor	0603	Kemet	C0603C563K1RACTU	$10.50	$0.11	USD
1	220k	Resistor	1206	TE Connectivity	CRGP1206F220K	$7.26	$0.07	USD
1	220k	Resistor	1206	TE Connectivity	CRGP1206F220K	$7.26	$0.07	USD
1	220k	Resistor	1206	TE Connectivity	CRGP1206F220K	$7.26	$0.07	USD
1	220k	Resistor	1206	TE Connectivity	CRGP1206F220K	$7.26	$0.07	USD
1	220k	Resistor	1206	TE Connectivity	CRGP1206F220K	$7.26	$0.07	USD
1	220k	Resistor	1206	TE Connectivity	CRGP1206F220K	$7.26	$0.07	USD
1	4.7u	Capacitor	1206	Murata Electronics	GRM31CZ72A475KE11L	$48.00	$0.48	USD
1	BAV99	Diode	SOT23	Nexperia	BAV99	$9.20	$0.09	USD
1	MM3Z12	Diode	SOD-323F	Diotec Semiconductor	MM3Z12	$6.20	$0.06	USD
1	BAV99	Diode	SOT23	Nexperia	BAV99	$9.20	$0.09	USD
1	CU3225K275G2	Varistor	3225	TDK	B72650M0271K072	$55.30	$0.55	USD
1	IPD65R190C7	Mosfet	DPAK	Infineon	IPD65R190C7ATMA1	$173.00	$1.73	USD
1	IPD65R190C7	Mosfet	DPAK	Infineon	IPD65R190C7ATMA1	$173.00	$1.73	USD
1	"unknow component"	"unknow component"	SOT323-5	"unknow component"	"unknow component"	$28.90	$0.29	USD
1	"unknow component"	"unknow component"	SOT323-5	"unknow component"	"unknow component"	$28.90	$0.29	USD
1	47	Resistor	0603	Vishay	CRCW060347R0JNEAC	$1.20	$0.01	USD
1	CD4093B	NAND	TSSOP14	Texas Instrument	CD4093BPWR	$59.80	$0.60	USD
1	HMHA2801	Optocoupler	MPF4	Onsemi	HMHA2801	$36.80	$0.37	USD
1	100k	Resistor	0603	Vishay	CRCW0603100KJNEAC	$1.00	$0.01	USD
1	1n	Capacitor	0603	Samsung Electro-Mechanics	CL10B102KC8NNWC	$2.60	$0.03	USD
1	PDTC144EE	Transistor	SOT416	Nexperia	PDTC144ET	$8.20	$0.08	USD
1	220k	Resistor	0603	Vishay	CRCW0603220KFKEAC	$1.30	$0.01	USD
1	56n	Capacitor	0603	Kemet	C0603C563K1RACTU	$10.50	$0.11	USD
1	220k	Resistor	1206	TE Connectivity	CRGP1206F220K	$7.26	$0.07	USD
1	220k	Resistor	1206	TE Connectivity	CRGP1206F220K	$7.26	$0.07	USD
1	220k	Resistor	1206	TE Connectivity	CRGP1206F220K	$7.26	$0.07	USD
1	220k	Resistor	1206	TE Connectivity	CRGP1206F220K	$7.26	$0.07	USD
1	220k	Resistor	1206	TE Connectivity	CRGP1206F220K	$7.26	$0.07	USD
1	220k	Resistor	1206	TE Connectivity	CRGP1206F220K	$7.26	$0.07	USD
1	4.7u	Capacitor	1206	Murata Electronics	GRM31CZ72A475KE11L	$48.00	$0.48	USD
1	BAV99	Diode	SOT23	Nexperia	BAV99	$9.20	$0.09	USD
1	MM3Z12	Diode	SOD-323F	Diotec Semiconductor	MM3Z12	$6.20	$0.06	USD
1	BAV99	Diode	SOT23	Nexperia	BAV99	$9.20	$0.09	USD
1	1M	Resistor	1206	Vishay	CRCW12061M00JNEAC	$2.10	$0.02	USD
1	1M	Resistor	1206	Vishay	CRCW12061M00JNEAC	$2.10	$0.02	USD
1	10mH	Inductor	Axial	TT Electronics	HM51-103KLF	$103.00	$1.03	USD
1	680n	Capacitor	Radial	Kemet	F461DB684J250	$63.20	$0.63	USD
1	47k	NTC	0805	Ametherm	SM08503395	$89.60	$0.90	USD
1	680p	Capacitor	0603	Kyocera AVX	06031C681KAT4A	$7.00	$0.07	USD
1	PCB 2Layers	29mm x 47mm x 1mm	100 pieces			$52.12	$0.52	USD
				TOTAL			**$17.12**	**USD**

- New BOM (Quoted prices per 100 pieces from Mouser, Digikey, PCB Way and TME Electronic components on Nov 24th, 2025)

Qty	Value	Part Function	Package	Supplier name	Supplier part number	Price (per 100)	Price	Currency
1	CU3225K150G2	Varistor	3225	TDK	B72650M0151K072	$55.30	$0.55	USD
1	STL18N65M5	Mosfet	PowerFLAT 5x6 HV	ST Micro	STL18N65M5	$231.00	$2.31	USD
1	STL18N65M5	Mosfet	PowerFLAT 5x6 HV	ST Micro	STL18N65M5	$231.00	$2.31	USD
1	TPSMB12CA-VR	TVS bidirectional	SMB	Littlefuse	TPSMB12CA-VR	$41.60	$0.42	USD
1	TPSMB12CA-VR	TVS bidirectional	SMB	Littlefuse	TPSMB12CA-VR	$41.60	$0.42	USD
1	47	Resistor	0603	Vishay	CRCW060347R0JNEAC	$1.20	$0.01	USD
1	CD4093B	NAND	TSSOP14	Texas Instrument	CD4093BPWR	$59.80	$0.60	USD
1	HMHA2801	Optocoupler	MPF4	Onsemi	FODM217D	$33.40	$0.33	USD
1	100k	Resistor	0603	Vishay	CRCW0603100KJNEAC	$1.00	$0.01	USD
1	1n	Capacitor	0603	Samsung Electro-Mechanics	CL10B102KC8NNWC	$2.60	$0.03	USD
1	220k	Resistor	0603	Vishay	CRCW0603220KFKEAC	$1.30	$0.01	USD
1	56n	Capacitor	0603	Kemet	C0603C563K1RACTU	$10.50	$0.11	USD
1	220k	Resistor	1206	TE Connectivity	CRGP1206F220K	$7.26	$0.07	USD
1	220k	Resistor	1206	TE Connectivity	CRGP1206F220K	$7.26	$0.07	USD
1	220k	Resistor	1206	TE Connectivity	CRGP1206F220K	$7.26	$0.07	USD
1	220k	Resistor	1206	TE Connectivity	CRGP1206F220K	$7.26	$0.07	USD
1	220k	Resistor	1206	TE Connectivity	CRGP1206F220K	$7.26	$0.07	USD
1	220k	Resistor	1206	TE Connectivity	CRGP1206F220K	$7.26	$0.07	USD
1	4.7u	Capacitor	1206	Murata Electronics	GRM31CZ72A475KE11L	$48.00	$0.48	USD
1	BAV99	Diode	SOT23	Nexperia	BAV99	$9.20	$0.09	USD
1	MM3Z12	Diode	SOD-323F	Diotec Semiconductor	MM3Z12	$6.20	$0.06	USD
1	BAV99	Diode	SOT23	Nexperia	BAV99	$9.20	$0.09	USD
1	CU3225K150G2	Varistor	3225	TDK	B72650M0151K072	$55.30	$0.55	USD
1	STL18N65M5	Mosfet	PowerFLAT 5x6 HV	ST Micro	STL18N65M5	$231.00	$2.31	USD
1	STL18N65M5	Mosfet	PowerFLAT 5x6 HV	ST Micro	STL18N65M5	$231.00	$2.31	USD
1	TPSMB12CA-VR	TVS bidirectional	SMB	Littlefuse	TPSMB12CA-VR	$41.60	$0.42	USD
1	TPSMB12CA-VR	TVS bidirectional	SMB	Littlefuse	TPSMB12CA-VR	$41.60	$0.42	USD
1	47	Resistor	0603	Vishay	CRCW060347R0JNEAC	$1.20	$0.01	USD
1	CD4093B	NAND	TSSOP14	Texas Instrument	CD4093BPWR	$59.80	$0.60	USD
1	HMHA2801	Optocoupler	MPF4	Onsemi	FODM217D	$33.40	$0.33	USD
1	100k	Resistor	0603	Vishay	CRCW0603100KJNEAC	$1.00	$0.01	USD
1	1n	Capacitor	0603	Samsung Electro-Mechanics	CL10B102KC8NNWC	$2.60	$0.03	USD
1	220k	Resistor	0603	Vishay	CRCW0603220KFKEAC	$1.30	$0.01	USD
1	56n	Capacitor	0603	Kemet	C0603C563K1RACTU	$10.50	$0.11	USD
1	220k	Resistor	1206	TE Connectivity	CRGP1206F220K	$7.26	$0.07	USD
1	220k	Resistor	1206	TE Connectivity	CRGP1206F220K	$7.26	$0.07	USD
1	220k	Resistor	1206	TE Connectivity	CRGP1206F220K	$7.26	$0.07	USD
1	220k	Resistor	1206	TE Connectivity	CRGP1206F220K	$7.26	$0.07	USD
1	220k	Resistor	1206	TE Connectivity	CRGP1206F220K	$7.26	$0.07	USD
1	220k	Resistor	1206	TE Connectivity	CRGP1206F220K	$7.26	$0.07	USD
1	4.7u	Capacitor	1206	Murata Electronics	GRM31CZ72A475KE11L	$48.00	$0.48	USD
1	BAV99	Diode	SOT23	Nexperia	BAV99	$9.20	$0.09	USD
1	MM3Z12	Diode	SOD-323F	Diotec Semiconductor	MM3Z12	$6.20	$0.06	USD
1	BAV99	Diode	SOT23	Nexperia	BAV99	$9.20	$0.09	USD
1	1M	Resistor	1206	Vishay	CRCW12061M00JNEAC	$2.10	$0.02	USD
1	1M	Resistor	1206	Vishay	CRCW12061M00JNEAC	$2.10	$0.02	USD
1	10mH	Inductor	Axial	TT Electronics	HM51-103KLF	$103.00	$1.03	USD
1	680n	Capacitor	Radial	Kemet	F461DB684J250	$63.20	$0.63	USD
1	47k	NTC	0805	Ametherm	SM08503395	$89.60	$0.90	USD
1	680p	Capacitor	0603	Kyocera AVX	06031C681KAT4A	$7.00	$0.07	USD
1	PCB 4Layers	70mm x 45mm x 1mm				$122.93	$1.23	USD
1	CU3225K150G2	Varistor	3225	TDK	B72650M0151K072	$55.30	$0.55	USD
1	STL18N65M5	Mosfet	PowerFLAT 5x6 HV	ST Micro	STL18N65M5	$231.00	$2.31	USD
1	STL18N65M5	Mosfet	PowerFLAT 5x6 HV	ST Micro	STL18N65M5	$231.00	$2.31	USD
1	TPSMB12CA-VR	TVS bidirectional	SMB	Littlefuse	TPSMB12CA-VR	$41.60	$0.42	USD
1	TPSMB12CA-VR	TVS bidirectional	SMB	Littlefuse	TPSMB12CA-VR	$41.60	$0.42	USD
1	47	Resistor	0603	Vishay	CRCW060347R0JNEAC	$1.20	$0.01	USD

1	CD4093B	NAND	TSSOP14	Texas Instrument	CD4093BPWR	$59.80	$0.60	USD
1	HMHA2801	Optocoupler	MPF4	Onsemi	FODM217D	$33.40	$0.33	USD
1	100k	Resistor	0603	Vishay	CRCW0603100KJNEAC	$1.00	$0.01	USD
1	1n	Capacitor	0603	Samsung Electro-Mechanics	CL10B102KC8NNWC	$2.60	$0.03	USD
1	220k	Resistor	0603	Vishay	CRCW0603220KFKEAC	$1.30	$0.01	USD
1	56n	Capacitor	0603	Kemet	C0603C563K1RACTU	$10.50	$0.11	USD
1	220k	Resistor	1206	TE Connectivity	CRGP1206F220K	$7.26	$0.07	USD
1	220k	Resistor	1206	TE Connectivity	CRGP1206F220K	$7.26	$0.07	USD
1	220k	Resistor	1206	TE Connectivity	CRGP1206F220K	$7.26	$0.07	USD
1	220k	Resistor	1206	TE Connectivity	CRGP1206F220K	$7.26	$0.07	USD
1	220k	Resistor	1206	TE Connectivity	CRGP1206F220K	$7.26	$0.07	USD
1	220k	Resistor	1206	TE Connectivity	CRGP1206F220K	$7.26	$0.07	USD
1	4.7u	Capacitor	1206	Murata Electronics	GRM31CZ72A475KE11L	$48.00	$0.48	USD
1	BAV99	Diode	SOT23	Nexperia	BAV99	$9.20	$0.09	USD
1	MM3Z12	Diode	SOD-323F	Diotec Semiconductor	MM3Z12	$6.20	$0.06	USD
1	BAV99	Diode	SOT23	Nexperia	BAV99	$9.20	$0.09	USD
1	CU3225K150G2	Varistor	3225	TDK	B72650M0151K072	$55.30	$0.55	USD
1	504M02QA100	Snubber		Knowles	504M02QA100	$1,474.00	$14.74	USD
1	HF49FD	Relay		Hongfa	HF49FD/012-1H12TB	$80.00	$0.80	USD
1	47	Resistor	0603	Vishay	CRCW060347R0JNEAC	$1.20	$0.01	USD
1	CD4093B	NAND	TSSOP14	Texas Instrument	CD4093BPWR	$59.80	$0.60	USD
1	HMHA2801	Optocoupler	MPF4	Onsemi	FODM217D	$33.40	$0.33	USD
1	100k	Resistor	0603	Vishay	CRCW0603100KJNEAC	$1.00	$0.01	USD
1	1n	Capacitor	0603	Samsung Electro-Mechanics	CL10B102KC8NNWC	$2.60	$0.03	USD
1	220k	Resistor	0603	Vishay	CRCW0603220KFKEAC	$1.30	$0.01	USD
1	56n	Capacitor	0603	Kemet	C0603C563K1RACTU	$10.50	$0.11	USD
1	220k	Resistor	1206	TE Connectivity	CRGP1206F220K	$7.26	$0.07	USD
1	220k	Resistor	1206	TE Connectivity	CRGP1206F220K	$7.26	$0.07	USD
1	220k	Resistor	1206	TE Connectivity	CRGP1206F220K	$7.26	$0.07	USD
1	220k	Resistor	1206	TE Connectivity	CRGP1206F220K	$7.26	$0.07	USD
1	220k	Resistor	1206	TE Connectivity	CRGP1206F220K	$7.26	$0.07	USD
1	220k	Resistor	1206	TE Connectivity	CRGP1206F220K	$7.26	$0.07	USD
1	4.7u	Capacitor	1206	Murata Electronics	GRM31CZ72A475KE11L	$48.00	$0.48	USD
1	BAV99	Diode	SOT23	Nexperia	BAV99	$9.20	$0.09	USD
1	MM3Z12	Diode	SOD-323F	Diotec Semiconductor	MM3Z12	$6.20	$0.06	USD
1	BAV99	Diode	SOT23	Nexperia	BAV99	$9.20	$0.09	USD
1	CU3225K150G2	Varistor	3225	TDK	B72650M0151K072	$55.30	$0.55	USD
1	504M02QA100	Snubber		Knowles	504M02QA100	$1,474.00	$14.74	USD
1	HF49FD	Relay		Hongfa	HF49FD/012-1H12TB	$80.00	$0.80	USD
1	47	Resistor	0603	Vishay	CRCW060347R0JNEAC	$1.20	$0.01	USD
1	CD4093B	NAND	TSSOP14	Texas Instrument	CD4093BPWR	$59.80	$0.60	USD
1	HMHA2801	Optocoupler	MPF4	Onsemi	FODM217D	$33.40	$0.33	USD
1	100k	Resistor	0603	Vishay	CRCW0603100KJNEAC	$1.00	$0.01	USD
1	1n	Capacitor	0603	Samsung Electro-Mechanics	CL10B102KC8NNWC	$2.60	$0.03	USD
1	220k	Resistor	0603	Vishay	CRCW0603220KFKEAC	$1.30	$0.01	USD
1	56n	Capacitor	0603	Kemet	C0603C563K1RACTU	$10.50	$0.11	USD
1	220k	Resistor	1206	TE Connectivity	CRGP1206F220K	$7.26	$0.07	USD
1	220k	Resistor	1206	TE Connectivity	CRGP1206F220K	$7.26	$0.07	USD
1	220k	Resistor	1206	TE Connectivity	CRGP1206F220K	$7.26	$0.07	USD
1	220k	Resistor	1206	TE Connectivity	CRGP1206F220K	$7.26	$0.07	USD
1	220k	Resistor	1206	TE Connectivity	CRGP1206F220K	$7.26	$0.07	USD
1	220k	Resistor	1206	TE Connectivity	CRGP1206F220K	$7.26	$0.07	USD
1	4.7u	Capacitor	1206	Murata Electronics	GRM31CZ72A475KE11L	$48.00	$0.48	USD
1	BAV99	Diode	SOT23	Nexperia	BAV99	$9.20	$0.09	USD
1	MM3Z12	Diode	SOD-323F	Diotec Semiconductor	MM3Z12	$6.20	$0.06	USD
1	BAV99	Diode	SOT23	Nexperia	BAV99	$9.20	$0.09	USD
TOTAL							**$65.40**	**USD**

C. SCHEMATIC DESIGN (NEW POWER BOARD)

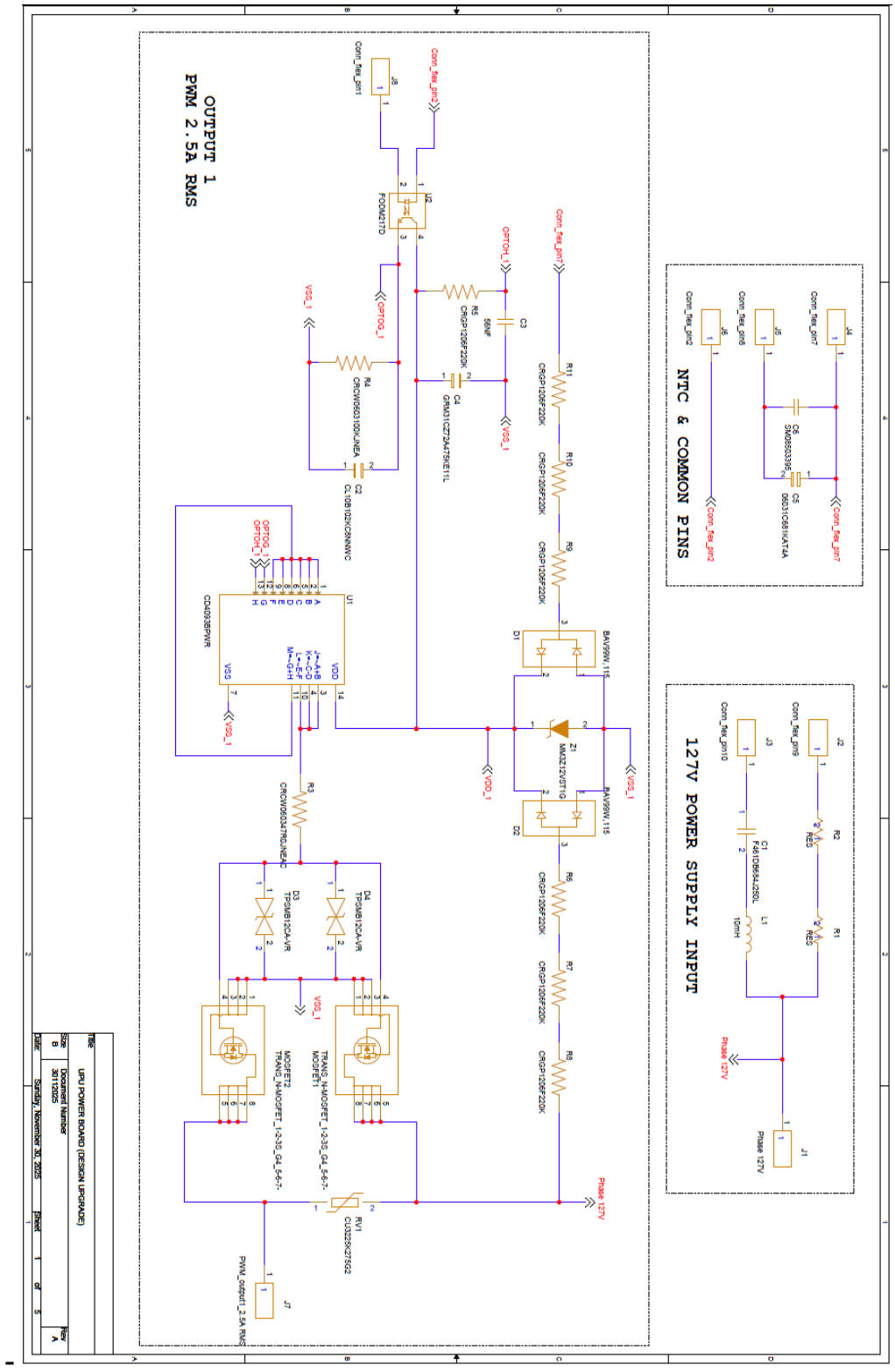

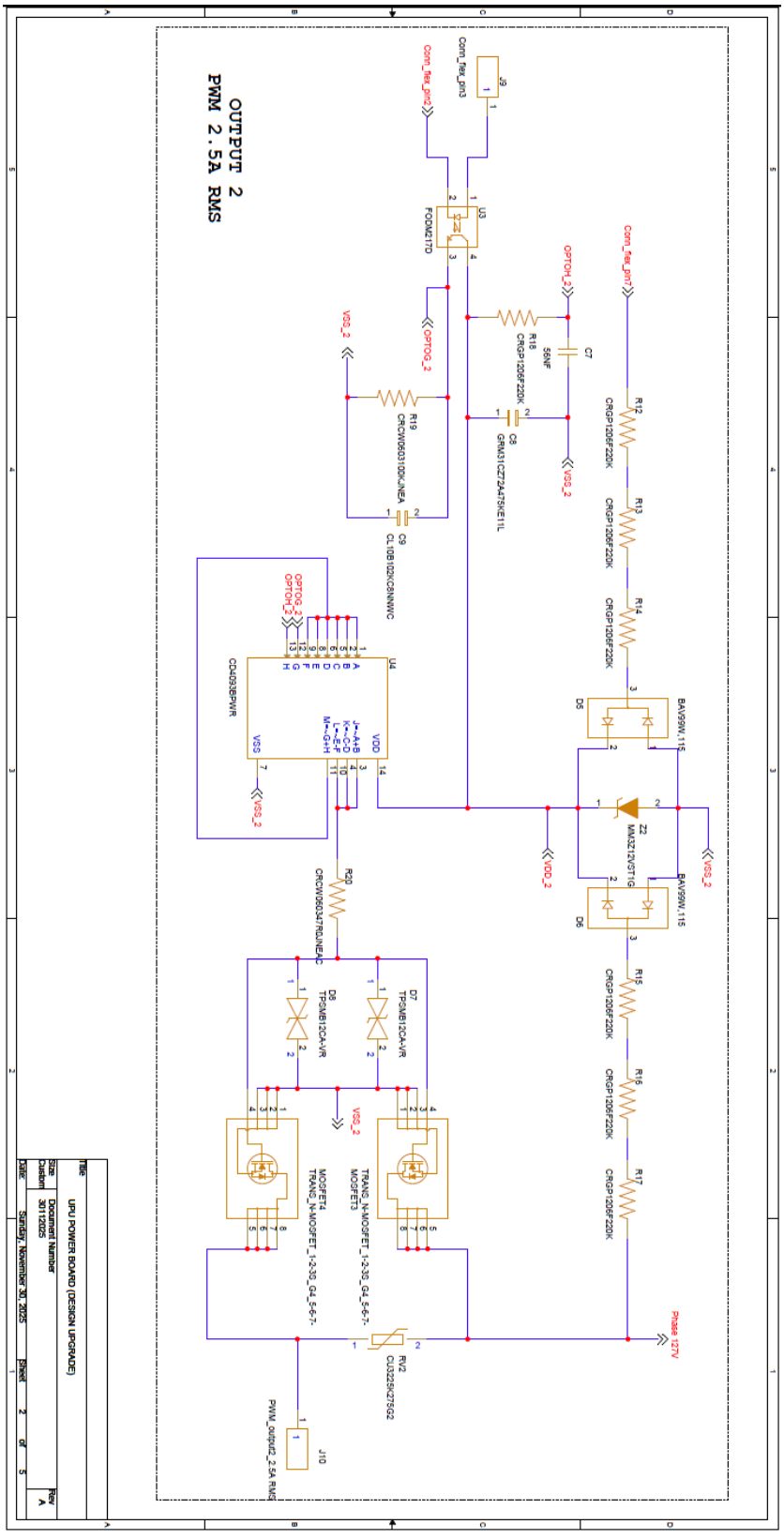
OUTPUT 2
PWM 2.5A RMS
Com_flex_pin3
Com_flex_pin7
J9
U3
FODM217D
OPTO4_2
OPTO5_2
VSS_2
R18
CRGP1206F220K
56NF
C7
C8
GRM31CZ72A475KE11L
R19
CRCW060310R0JNEA
C9
CL10B102KCBNNWC
R12
R13
R14
R15
R16
R17
D5
D6
BAV99W,115
Z3
MMSZ12VST1G
VDD_2
U4
CD4093BPWR
R20
CRCW0603470RJNEAC
D8
TPSMB12CA-VR
D7
TPSMB12CA-VR
MOSFET4
TRANS_N-MOSFET_1-2-3S_G4_5-6-7-
MOSFET3
TRANS_N-MOSFET_1-2-3S_G4_5-6-7-
RV2
CU3225K275G2
Phase 127V
J10
PWM_OUTPUT2_2.5A_RMS
Title
UPU POWER BOARD (DESIGN UPGRADE)
Size
Custom
Document Number
30112025
Rev
A
Date:
Sunday, November 30, 2025
Sheet
2
of
5

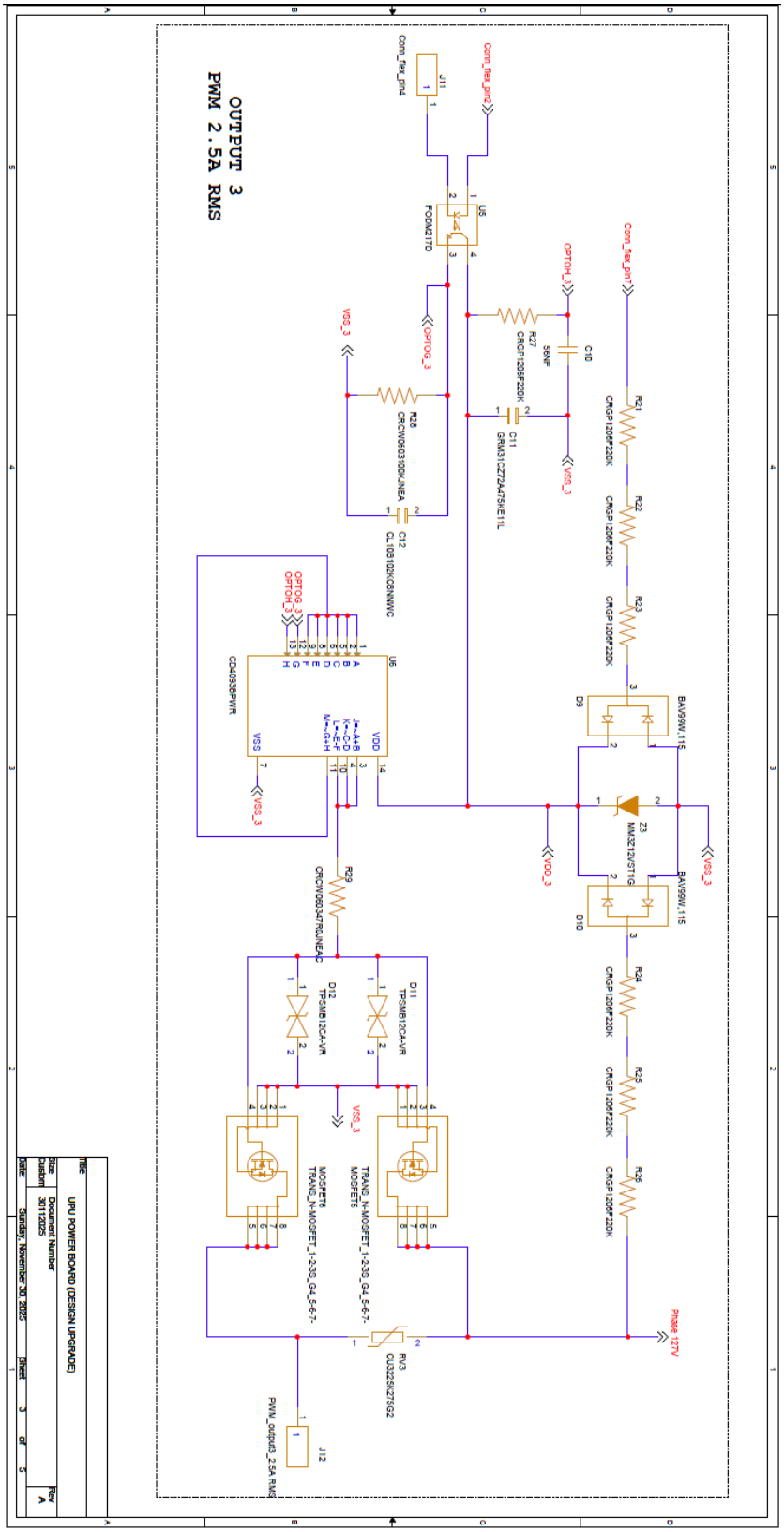
OUTPUT 3
PWM 2.5A RMS
Comm_flex_pin4
Comm_flex_pin7
J11
U5
FODM217D
OPTO4_3
OPTO3_3
R27
CRGP1206F220K
56NF
C10
C11
GRM31CZ72A475KE11L
R21
R22
R23
R24
R25
R26
CRGP1206F220K
R28
CRCW060310R0JNEA
C12
CL10B102KQ8NNWC
D9
D10
BAV99W,115
Z3
MMSZ12VST1G
VDD_3
VSS_3
U6
CD4093BPWR
R29
CRCW060347R0JNEAC
D11
D12
TPSMB12CA-VR
MOSFET5
MOSFET6
TRANS_N-MOSFET_1-2-3S_G4_5-6-7-
RV3
CU3225K275G2
Phase 120V
J12
PWM_outputs3_2.5A RMS
Title
UPU POWER BOARD (DESIGN UPGRADE)
Size
Custom
Document Number
30112025
Rev
A
Date:
Sunday, November 30, 2025
Sheet
3
of
5

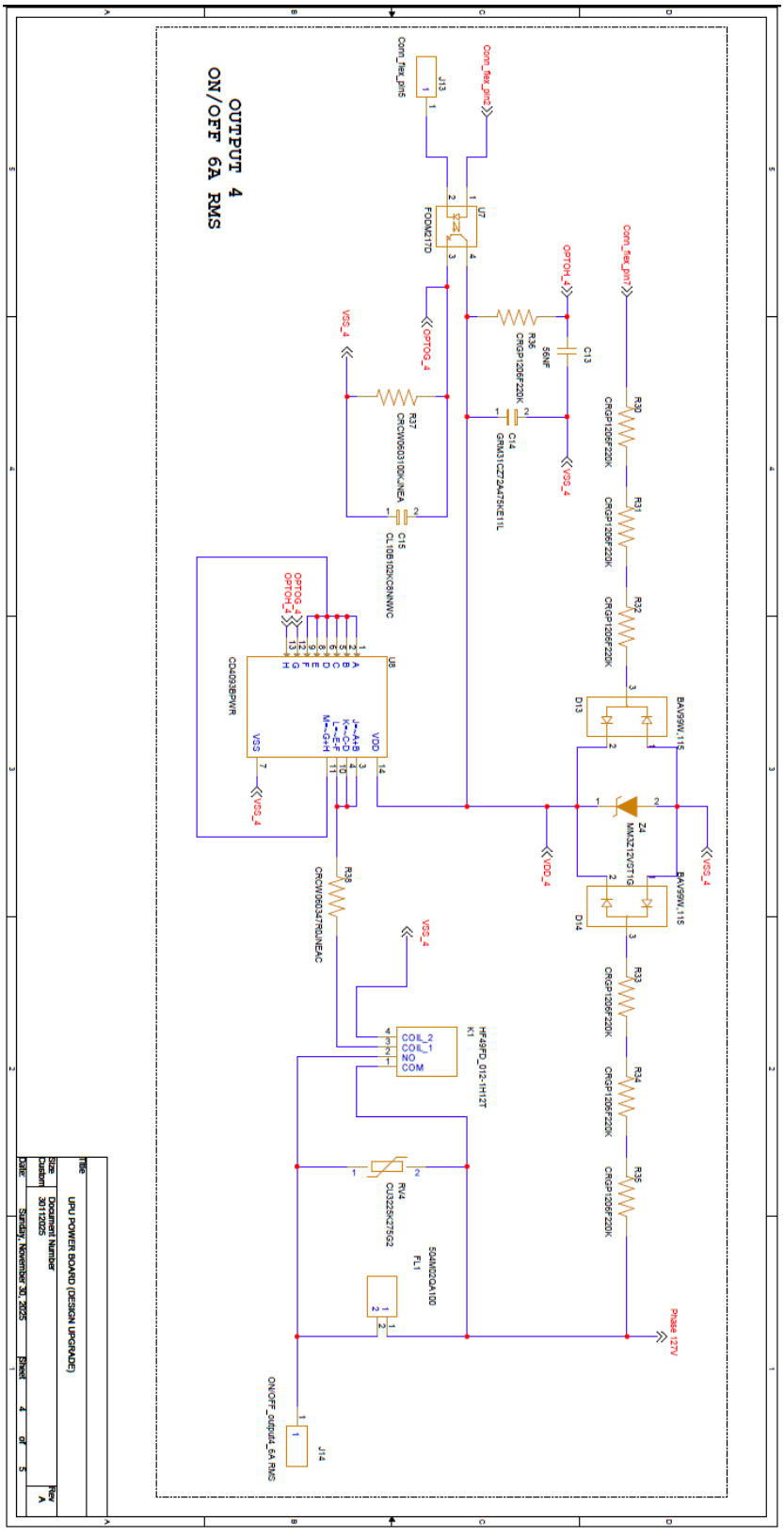
OUTPUT 4
ON/OFF 6A RMS
Conn_flex_pin5
Conn_flex_pin6
Conn_flex_pin7
J13
U7
FODM217D
OPTOG_4
OPTOH_4
VSS_4
VDD_4
R36
CRGP1206F220K
56NF
C13
C14
GRM31CF72A475KE11L
R37
CRCW060310KJNEA
C15
CL10B102KC8NNWC
R30
R31
R32
R33
R34
R35
CRGP1206F220K
D13
D14
BAV99W,115
Z4
MMSZ12VST1G
U8
CD4053BPWR
R38
CRCW06034R70JNEAC
K1
HF46FD_012-1H12T
COIL_2
COIL_1
NO
COM
RV4
CU3225K275G2
SGAM2GDA100
FL1
Phase_127V
J14
ON/OFF_output4_6A RMS
Title
UPU POWER BOARD (DESIGN UPGRADE)
Size
Custom
Document Number
30112025
Rev
A
Date:
Sunday, November 30, 2025
Sheet
4
of
5

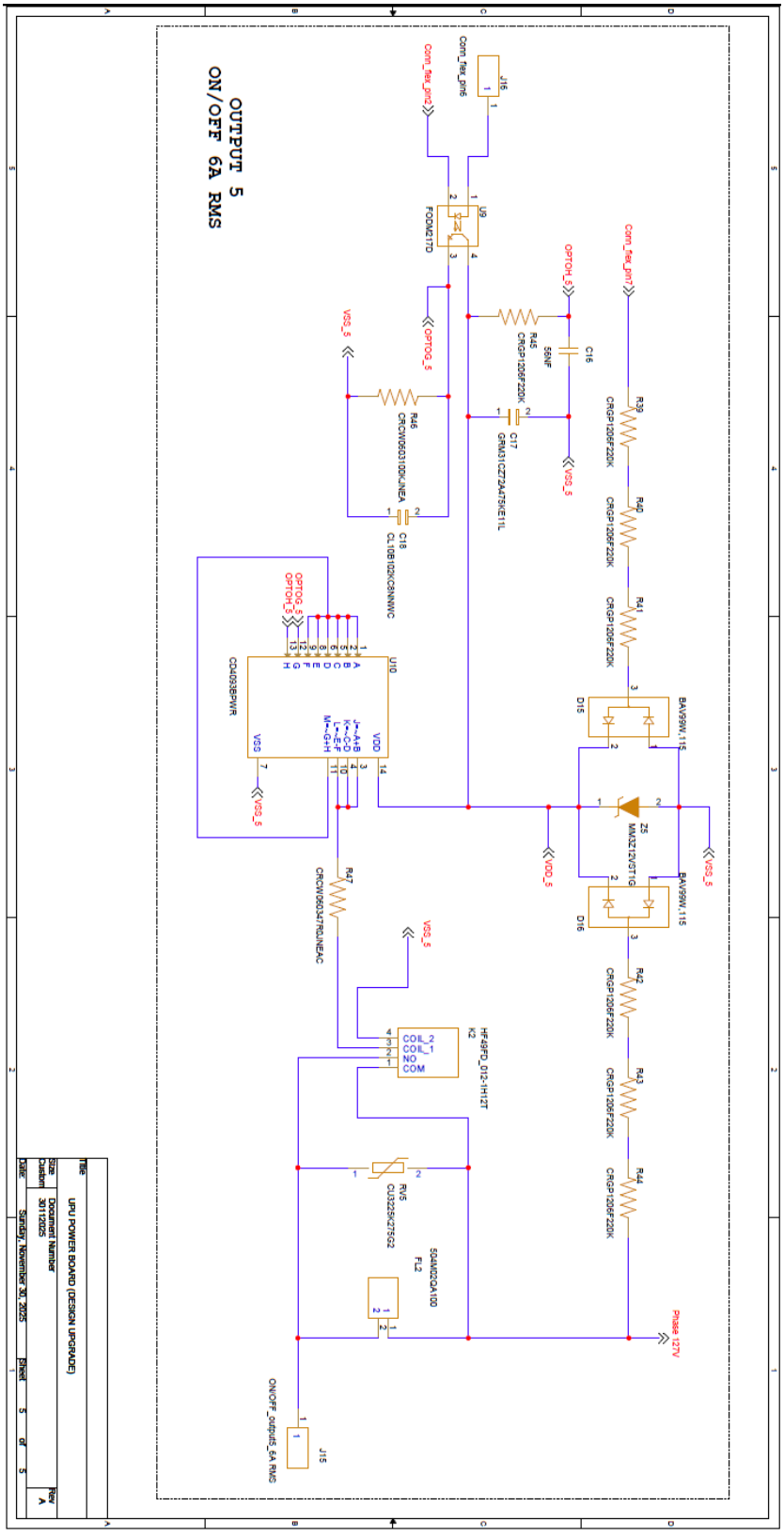
OUTPUT 5
ON/OFF 6A RMS
Comm_flex_pin6
Comm_flex_pin7
J16
U9
FODM217D
OPTOG_5
OPTOH_5
R45
CRGP1206F220K
56NF
C16
C17
GRM31CZ72A475KE11L
VSS_5
R46
CRCW060310R0JNEA
C15
CL10B102KCBNNWC
R39
R40
R41
D15
BAV99W,115
Z5
MMSZ12V3T1G
D16
R42
R43
R44
VDD_5
U10
CD4093BPWR
OPTOG_5
OPTOH_5
R47
CRCW060347R0JNEAC
HF49FD_012-1H12T
K2
COIL_2
COIL_1
NO
COM
RV5
CU3225K275G2
5GM020A100
FL2
Phase 127V
J15
ON/OFF_OUTPUT5_6A RMS
Title
UPU POWER BOARD (DESIGN UPGRADE)
Size
Custom
Document Number
30112025
Rev
A
Date:
Sunday, November 30, 2025
Sheet
5
of
5

References

[1] I. Kg, “Der High-End Installationsbus.” Apr. 2015.

[2] “What is information technology? | Definition from TechTarget,” Search Data Center. Accessed: Apr. 06, 2025. [Online]. Available: https://www.techtarget.com/searchdatacenter/definition/IT

[3] L. Molina González, *Instalaciones domoticas*, 2010th ed. Madrid: McGraw-Hill/Interamericana de España, S.L.

[4] M. Karlen and C. Spangler, “Chapter 7: Lighting Controls,” in *Lighting Design Basics*, Fouth Edition., Hoboken, New Jersey: John Wiley & Sons, 2024.

[5] E. Zwemmer and S. Broekema, “8.4 Assigment 4 - Dimming/Control/Savings,” in *DALI Basic cource*, 2nd edition., The Netherlands: InstaVer Systems B.V., 2025, p. 179.

[6] “Leading Edge vs. Trailing Edge Dimming | Top Designer LED Lighting Manufacturer Company in New York.” Accessed: Apr. 18, 2025. [Online]. Available: https://rbw.com/blog/leading-edge-vs-trailing-edge-dimming

[7] R. Mente, “Addressing space and efficiency in high-power applications,” *Power Systems Design*, p. 14, Sept. 2014.

[8] D. Graovac, M. Pürschel, and A. Kiep, “MOSFET Power Losses Calculation Using the Data-Sheet Parameters, Application Note.” Infineon Technologies, July 2006.

[9] “Introduction to the MOSFET temperature coefficient α.” Accessed: May 03, 2025. [Online]. Available: https://community.infineon.com/t5/Knowledge-Base-Articles/Introduction-to-the-MOSFET-temperature-coefficient-%CE%B1/ta-p/939093

[10] W. McDaniel, “MOSFET Thermal Characterization in the Application.” Vishay Siliconix, May 2001.

[11] “Safety Precautions of General Purpose Relays Cautions for General Purpose Relays | OMRON Industrial Automation.” Accessed: Nov. 14, 2025. [Online]. Available: https://www.ia.omron.com/product/cautions/36/safety_precautions.html

[12] E. D. N. Staff, “A hands-on guide for RC snubbers and inductive load suppression,” EDN. Accessed: Nov. 16, 2025. [Online]. Available: https://www.edn.com/a-hands-on-guide-for-rc-snubbers-and-inductive-load-suppression/

[13] W. Instruments, “Components of Relay Contact Protection | Digital Panel Meter,” Weschler Instruments. Accessed: Nov. 16, 2025. [Online]. Available: https://www.weschler.com/blog/relay-contact-protection/

[14] “Understanding the Working Principles and Applications of Metal Oxide Varistors.” Accessed: Nov. 16, 2025. [Online]. Available: https://www.ic-components.com/blog/understanding-the-working-principles-and-applications-of-metal-oxide-varistors.jsp

[15] "Frequently Asked Questions - Spark Quenchers," Okaya Electric America. Accessed: Nov. 16, 2025. [Online]. Available: https://okaya.com/products/noise-products/spark-quenchers/spark-quencher-faq/

[16] R. Co, "TO252 Package Thermal Resistance Information," no. 64, 2022.